Forecast models of coffee leaf rust symptoms and signs based on identified microclimatic combinations in coffee-based agroforestry systems in Costa Rica

Isabelle Merle, Philippe Tixier, Elías de Melo Virginio Filho, Christian Cilas, Jacques Avelino

Forecast models of coffee leaf rust symptoms and signs based on identified microclimatic combinations in coffee-based agroforestry systems in Costa Rica

Isabelle Merle [a, b, *], Philippe Tixier [c, d], Elías de Melo Virginio Filho [e], Christian Cilas [b, f], and Jacques Avelino [a, b, e, g]

[a] CIRAD, UPR Bioagresseurs, 30501 Turrialba, Costa Rica

[b] Bioagresseurs, Univ Montpellier, CIRAD, Montpellier, France

[c] CIRAD, UPR GECO, F-34398 Montpellier, France

[d] GECO, Univ Montpellier, CIRAD, Montpellier, France

[e] CATIE, 7170, Cartago, Turrialba, 30501, Costa Rica

[f] CIRAD, UPR Bioagresseurs, F-34398 Montpellier, France

[g] IICA AP. 55, 2200 Coronado, San José, Costa Rica

Corresponding author**:** E-mail:isabelle.merle@protonmail.com

ABSTRACT

Coffee leaf rust is a polycyclic disease that causes severe epidemics impacting yield over several years. For this reason, since the 1960s, more than 20 models have been developed to predict different indicators of the disease's development and help manage it. In existing models, standardized periods of influence of the meteorological predictors of the disease are determined *a priori,* based on strong assumptions. However, the appearance of a symptom or sign can be influenced by complex combinations of meteorological variables acting at different times and for

different durations. In our study, we monitored a total of 5400 coffee leaves during a year and a half, in different agroforestry systems, in order to detect the onset dates of the disease symptoms, such as lesion emergence, and signs, such as sporulation and infectious area increase. In these agroforestry systems, we also recorded microclimate. We statistically identified the complex combinations of microclimatic variables responsible for changes in lesion status to construct three models predicting lesion emergence probability, lesion sporulation probability and growth of its infectious area. Our method allowed the identification of different microclimatic variables that fit well with the knowledge about the coffee leaf rust biology. Minimum air temperature from 20 to 18 days before a lesion emergence explained the status change from healthy to emergence of visible lesion, possibly because the short germination phase is stimulated by low temperatures. We also found a unimodal effect of rainfall over a period of 10 days, 33 days before lesion emergence, with a maximum at 10 mm. Below this threshold, uredospore dispersal is efficient, increasing the lesion appearance probability; above this threshold, wash-off effects on uredospores probably occurs, decreasing the probability of lesion emergence. In addition, we identified microclimatic variables whose influence on coffee leaf rust had not been described before. These variables are likely to be involved in the internal development phases of the disease in the coffee leaves: (1) unimodal effects of maximum air temperature in different periods on sporulation and infectious area growth (2) positive and unimodal effects of rainfall in different periods on sporulation and (3) a negative effect of leaf thermal amplitude in different periods on lesion emergence, sporulation and infectious area growth. Although these models do not provide predictors of the level of disease attack, such as incidence, they provide valuable information for warning systems and for mechanistic model development. These models could also be used to forecast risks of infection, sporulation and infectious area growth and help optimize treatment recommendations.

Keywords: *Hemileia vastatrix*, *Coffea arabica*, weather-based statistical modeling, daily temperature, daily rainfall

1. Introduction

The anticipation of disease outbreaks requires knowledge of the drivers that trigger them. This knowledge can then be used to develop decision-support tools to assist farmers and thus reduce risks (Krause and Massie, 1975). Forecasting the risk of an epidemic is even more important if this epidemic leads to economic and social crises due to multiyear repercussions, as in the case of perennial crops (Cerda et al., 2017) and if producers are highly vulnerable. This was the case in Central America in 2012 when a severe epidemic of coffee leaf rust caused the loss of about 20% of Arabica coffee production and resulted in the declaration of a state of emergency in three countries in the region (Avelino et al., 2015). In response to this crisis, immediate measures for damage assessment, plantation rehabilitation and stakeholder training were implemented in 2013 as part of a regional project led by the Instituto Interamericano de Cooperación para la Agricultura (IICA) and Programa Cooperativo Regional para el Desarrollo Tecnológico y Modernización de la Caficultura (PROMECAFE) in collaboration with coffee-related institutes in the region. This project was financially supported by the European Union from 2017 through the Central American Program for the Integral Management of Coffee Rust (PROCAGICA), having among its objectives the development of an early warning system for the region based on surveillance and coffee leaf rust forecasting. Despite the influence of economic and social factors on plant disease outbreaks (Almeida, 2018), meteorological anomalies were considered as one of the main triggering factors of the 2012 coffee leaf rust epidemic (Avelino et al., 2015). However,

71 predicting disease development remains a challenge, even when focusing on meteorological
72 variables (Cunniffe et al., 2015), and different modeling approaches can be used to develop
73 predictive models. These approaches are often grouped into three categories: statistical models,
74 mechanistic models and machine learning models (Siettos and Russo, 2013). The choice of an
75 approach depends on the purpose of the model, the knowledge available on the disease and
76 disease detection difficulties.

77 Statistical models depend on database analysis to describe the relationships between
78 environmental conditions and the development of the disease characterized by symptoms, visible
79 disease effects on the plant such as a chlorosis, and signs, physical evidence of the pathogen such
80 as spores. These models thus have a domain of definition and are not easily generalizable.
81 Mechanistic models have an explanatory purpose since they use equations describing the
82 different stages of the disease's development (de Wolf and Isard, 2007). These models are
83 therefore generalizable but require a significant amount of knowledge on the biology of the
84 pathogen and substantial work for parameterization purposes. Finally, machine learning models
85 make it possible to take a larger number of variables and their combinations into account for
86 prediction but must be developed based on a learning process with a very large database. Most
87 machine learning algorithms are considered as so-called "black box" systems, too complex to
88 provide a biological explanation of the effects of predictors (Rudin 2019) and often limiting the
89 user's ability to understand the results obtained (Krause and Massie, 1975).

90 Another important difference between the mechanistic approach and the other approaches for
91 developing weather-based models is that statistical models and machine learning models require
92 assumptions on the periods of action of these meteorological variables. In the field, monitoring
93 the development of plant diseases is based on the observation of symptoms and signs and the
94 calculation of indicators such as incidence and severity, which depend on both the development

of the disease and its host (Ferrandino, 2008). These variables are the result of several phases of the pathogen's development cycle. For example, for a coffee rust lesion to appear on a leaf, the fungus has to complete uredospore dispersal, deposition on the upper surface of the leaf, migration to the under surface, germination, germinative tube growth, apressorium formation to enter the leaf via a stomata and tissue colonization. Since these phases have varying durations and occur at different times, the influencing meteorological variables should affect disease at different times and during varying durations. This is even truer when considering disease descriptors such as incidence and severity that include the host plant dynamic, itself under the influence of meteorological variables.

In the case of coffee leaf rust, the first proposed models were multiple linear regressions between the average of minimum and maximum temperatures over incubation times (Kushalappa and Martins, 1980) or disease latency (Kushalappa and Martins, 1980; Santacreo et al., 1983; Tronconi et al., 1995). Because these experiments were based on inoculations, it might be logical not to consider variables such as rain or humidity driving uredospore dispersal, deposition and germination phases. These equations were simple but different from one site to another, indicating that they were not generalizable. These equations also considered linear effects of temperature, while controlled studies had already shown several unimodal effects of temperature on disease development (Kushalappa et al., 1983; Nutman et al., 1963). Subsequently, the models built incorporated a wide range of meteorological variables, sometimes comparing the influence of several periods (Alfonsi et al., 1974; Kushalappa, 1981; Pinto et al., 2002) but not carrying out a complete exploration of all the possible periods (Table 1). However, these studies had revealed the importance of choosing the periods of influence of meteorological variables. In addition, variables characterizing the host and quantifying the inoculum stock were considered as a way for model improvement. Further, to improve the models, incidence curves were linearized in

119 order to estimate the apparent infection rate of coffee leaf rust and then study the influence of
120 weather conditions on this rate (Pedro, 1983). In those years, the most advanced model was built
121 by Kushalappa et al. (1983, 1984). These authors developed a semi-mechanistic model in which
122 the necessary conditions for the development of monocyclic processes were quantified and
123 summarized in a single synthetic variable to explain the growth rate of the disease. The final
124 modeling step was still a regression with unimodal effects of the dependent synthetic variable on
125 the growth rate. The models developed produced recommendations regarding the appropriate
126 dates of fungicide sprays (Kushalappa et al., 1986). The implementation of this modeling
127 approach in Mexico led to different models from those obtained in Brazil, indicating once again
128 their instability (Holguín, 1987).
129 Since 1991, most studies have focused on predicting the incidence of the disease or the
130 infection risk rather than variables reflecting the different phases of rust development (Table 1).
131 Since the 2000s, most models have been generated using decision trees (Avelino et al., 2006) and
132 machine learning methods such as the support vector machine (Luaces et al., 2010), neural
133 networks (Pinto et al., 2002), decision trees (Meira et al., 2008, 2009), fuzzy decision trees
134 (Cintra et al., 2011) and Bayesian networks (Perez-Ariza et al., 2012). These modeling
135 approaches have enabled inclusion of a larger number of variables (Table 1), particularly
136 cropping practices such as fertilization and fungicide sprays (Corrales et al., 2016, 2015).
137 However, in all cases, the periods during which the meteorological variables were considered to
138 explain the disease were defined *a priori,* based on strong assumptions: monthly averages of
139 meteorological variables were chosen that did not reflect the short duration of certain stages of
140 the fungus's development. One recent study revisited mechanistic approaches, inspired by
141 survival analysis through calculation of instantaneous risk averages as a function of
142 meteorological variables (Bebber et al., 2016). Another recent study focusing on coffee leaf rust

143 prediction used the same concept of linearization of coffee leaf rust incidence used by
144 Kushalappa in 1981 and Pedro in 1983 to study the effect of three possible periods of influence of
145 meteorological variables (Hinnah et al., 2018) (Table 1).

146 We propose that improving the accuracy of prediction models does not necessarily require
147 taking more variables into account but rather identifying the precise combinations of
148 meteorological variables that cause onset of symptoms and signs. This approach would help us
149 arrive at a model with a balance between the simplicity to facilitate its use and the complexity to
150 provide sufficient precision. For coffee-based agroforestry systems, another point of
151 improvement in prediction accuracy is to understand how shade modifies the microclimatic
152 drivers of coffee leaf rust development, as meteorological variables are monitored by stations in
153 full sunlight. Few of the studies cited have considered the effect of shading in their model
154 (Avelino et al., 2006; Corrales et al., 2016, 2015; de Moraes et al., 1976). This is certainly due to
155 the major modernization of coffee plantations after the 1970s that led to the conversion of many
156 diversified agroforestry systems into monoculture systems, as in Brazil (Jha et al., 2014).
157 However, agroforestry is considered as a necessary practice in the future to cope with climate
158 change: it buffers extreme temperatures and reduces soil moisture fluctuations, for example (Lin
159 et al., 2007). Better understanding shade effects on microclimate could be useful to select
160 appropriate shade trees that help cope with climate change and regulate coffee leaf rust, if the
161 critical microclimatic variables and periods of influence of the microclimate were determined.

162 In our study, we tried to determine, without using *a priori* assumptions, which combinations
163 of microclimatic variables are responsible for the onset of coffee leaf rust symptoms and signs.
164 We applied a method developed in Bugaud et al. (2015), inspired by the Window Pane approach
165 introduced by Coakley and Line (1982), and already used to find the microclimatic periods that
166 influence abundance of banana thrips (Carval et al., 2015), pineapple acidity (Dorey et al., 2016)

or the onset of symptoms and signs of cocoa moniliasis (Leandro-Muñoz et al., 2017). These identified microclimatic variables were used to build three models: risks of lesion occurrence, sporulation and infectious area growth. The separation into several models had the benefit of simplifying the interpretation of the microclimatic combinations identified as well as predicting specific risks that imply different recommendations in terms of chemical control.

2. Materials and methods

2.1. Field locations

To observe a large range of microclimatic conditions, the trial was set up in coffee plots located in experimental sites distributed in a gradient of three altitudes over a 15-month period, from May 2017 to July 2018 The first site was the long-term trial of coffee-based agroforestry systems established by the Tropical Agricultural Research and Higher Education Center (CATIE, Centro Agronómico Tropical de Investigación y Enseñanza) in Turrialba, Costa Rica (9º53´44´´ latitude north, 83º40´7´´ longitude west) at an altitude of 600 m.a.s.l. The second site was a coffee-based agroforestry plot established by the Costa Rican Coffee Institute (ICAFE, Instituto del Café de Costa Rica) in Barva de Heredia, Costa Rica (10º2´9´´ latitude north, 84º8´11´´ longitude west) at an altitude of 1180 m.a.s.l. The third site was located in the plantation of a coffee grower living in Aserrí (9º50´54´´ latitude north, 84º6´0´´ longitude west), at an altitude of 1500 m.a.s.l., that trial beginning in September 2017, four months later than the others.

2.2. Experimental design

188 The trial was carried out on four plots: two in Turrialba, one in Heredia and one in Aserrí. The
189 two selected plots in Turrialba had the same agronomic management except for the agroforestry
190 practice, which offered different microclimatic conditions: one exposed to full sunlight; the other,
191 in an agroforestry system based on poró (*Erythrina poeppigiana)*. The plots located in Heredia
192 and Aserrí were also agroforestry systems, based on *E. poeppigiana* in Heredia and *E.*
193 *poeppigiana* combined with trees of the citrus family in Aserrí. In each plot, the coffee variety
194 planted was susceptible to most rust races and was managed without fungicides to monitor
195 natural behavior of coffee leaf rust. Each plot consisted of a minimum of six rows of coffee
196 plants, with 2 m between rows and a dozen coffee plants per row, with 1-m spacing. To avoid a
197 potential border effect, we selected the six central plants of the three central rows of each plot to
198 monitor the coffee leaf rust, totaling 18 coffee plants per plot. In January 2018, in the plots
199 located in Turrialba and Heredia, most of the selected plants were exhausted and deteriorated by
200 coffee leaf rust so were replaced by new ones. Since they were selected later, in September 2017,
201 the coffee plants of the plot in Aserrí were conserved for the 2018 monitoring. As shown in Fig.
202 1, the Heredia and Aserrí sites, under Pacific influence, faced a dry season from January to April
203 2018, while Turrialba site, under Caribbean influence, did not experience a significant dry season
204 during the experiment. On average, higher elevation sites were those where the lowest daily
205 minimum and maximum temperatures were measured.
206
207 **2.3. Field monitoring of coffee leaf rust symptoms and signs and inoculum stock assessment**
208 Every month, three branches per coffee plant (one branch in each of three coffee plant strata)
209 were selected and, from each branch, a node of young healthy leaves was labeled. This helped us
210 renew the stock of healthy leaves periodically. These selected pairs of leaves were then observed

211 weekly over a two-month period and photographed weekly from the onset of the first visible
212 symptom of the disease. The photographs were then analyzed by image processing with the
213 ImageJ software (Schindelin et al., 2015) (Fig. 2). Thanks to image processing analysis, we were
214 able to measure the lesion surfaces (symptoms and signs), from a size of 0.001 cm². This method
215 allowed a nondestructive monitoring of lesions over time and thus to record the history of each
216 lesion: the week it was detected, the week the first uredospores appeared, the size of its infectious
217 area each week. Finally, focusing on lesions rather than measuring indicators such as incidence
218 and severity allowed us to avoid the effects of host growth dynamics on the disease. Because
219 previous studies have shown that coffee fruit load can affect the leaf physiological resistance to
220 the fungus (Eskes and Souza 1981), we counted the number of fruiting nodes of each coffee plant
221 studied.

222 Each month, to estimate the inoculum amount present in the plot, we selected 18 branches
223 different from those used for coffee leaf rust symptoms and signs: one per selected coffee plant
224 and six branches per foliar stratum. On these branches, every leaf with coffee leaf rust lesions
225 showing uredospores was photographed. The rust area with uredospores was measured using the
226 ImageJ software. The total area per branch was calculated and averaged over the 18 branches
227 selected in each plot. This average was considered as a proxy for inoculum stock (Kushalappa,
228 1981; Merle et al., 2019).

229

230 **2.4. Microclimatic data recording**

231 Microclimate data were recorded using Campbell CR1000 (Campbell Scientific) data loggers
232 placed in the center of each of the four experimental plots. Each station was equipped with a data
233 logger connected to the following nine sensors:

- a rain gauge placed 2 m high and far from shade trees (TE525MM, accuracy 0.1 mm),
- an air temperature and relative humidity sensor positioned at 1.5 m high (HMP45C),
- four leaf wetness sensors at 1.2 m high and oriented in four different directions (Dielectric LWS),
- three T-type thermocouples (copper/constantan) giving the average temperature of three leaves each, chosen in three coffee plants and three different strata in each coffee plant (Miller, 1971).

Climatic data were recorded every five seconds by the sensors and their minimum, maximum and average values were stored every 30 minutes. Data were retrieved weekly from the data loggers using PC200W 4.5 Datalogger Support Software (Campbell Scientific).

2.5. Variables description

A total of 5400 leaves were monitored over all the 2-month periods, from May 2017 to July 2018. Among the total of appeared coffee leaf rust lesions, 95% ranked from the first to 25th lesion on a leaf. We therefore considered that 25 sites per leaf were available for coffee leaf rust lesion emergence. On each of the monitoring dates, each new lesion implied a change in status for a site from "healthy" to "infected." Once the lesion appeared, this site was no longer available on the following dates because it could not become infected again. The variable presence or absence of a new coffee leaf rust lesion per foliar site (*NewLesion*) was used as a response variable to build a model forecasting the lesion emergence probability per foliar site (Fig. 2). That means that at leaf scale, the predicted number of new lesions emerged is equal to this probability multiplied by the 25 foliar sites. The date of emergence of each lesion was used to compute the lesion's age, indicated in days but with a weekly accuracy due to the monitoring frequency

(*LesionAge*). At each monitoring date, a lesion with no uredospores had the possibility to change its status from "infected" to "infectious." The variable presence or absence of uredospores (*Sporulation*) on the lesions was used to build a model forecasting the probability of uredospore emergence (Fig. 2). The last model aimed to predict the infectious area (*InfectiousArea*) of the lesions. In order to reduce the error about the date of site status change, we considered that this date was the middle date between the date when the change was observed and the previous monitoring date.

These three variables describing coffee leaf rust development were explained as a function of these basic daily microclimatic variables: air minimum temperature, maximum temperature and thermal amplitude (*TaMin*, *TaMax*, *TaAmp*, respectively) as well as coffee leaf minimum temperature, maximum temperature and thermal amplitude (*TcMin*, *TcMax* and *TcAmp* respectively), relative humidity amplitude (*RHAmp*), total rainfall (*Rainfall*), rainfall duration (*FreqRain*) and leaf wetness duration from 6 a.m. to 11 a.m. (*FreqLW6to11*) and from noon to 6 p.m. (*FreqLW12to18*) (Table 2). By night, the leaves were always wet in our study sites because of dew. That is why we did not consider leaf wetness duration during the night. In addition, we chose to study the morning and the afternoon separately for leaf wetness to better consider the preinfectious processes: germination usually starts in the late afternoon and continues during night, and appresorium and penetration into the leaf occur soon in the morning (Rayner, 1961). Additional variables were measured because of their known effect on coffee leaf rust development: the average inoculum stock per branch at plot level, estimated weekly by linear interpolation from monthly data (*Inoculum*), the age of the lesions (*LesionAge*), the coffee leaf stratum that marked leaves belonged to (*LeafStratum*) and the number of fruiting nodes per coffee plant (*PlantFruitLoad*) (Table 2).

2.6. Statistical analysis

We performed a two-step analysis. For each microclimatic variable (*MicroclimVar*), we first needed to identify which periods better explained each of the three studied dependent variables: *NewLesion*, *Sporulation* and *InfectiousArea*. A period is defined by a duration (D) and a time before status change (T) (from a healthy foliar site to the emergence of a lesion, from a latent lesion to an infectious lesion, from the past infectious area to the current infectious area). The method used described by Bugaud et al. in 2015, proceeds as follows: (1) we calculated, over all the possible periods (T ranges from 1 to n and, for each time T, D ranges from 1 to T), the explanatory microclimatic variables $MicroclimVar_{TxDy}$, defined as the daily averaged microclimatic variable (Table 2) over a *y*-days period starting *x* days before the symptom or sign onset (2) each of these explanatory variables was included in a generalized linear model (GLM) to explain *NewLesion*, *Sporulation* and *InfectiousArea* with different distributions depending on the dependent variable (see Eqs. 1, 2 and 3); for rainfall and temperatures, which generally have a nonlinear effect, we tested their unimodal form; (3) explanation level provided by the variables was then assessed by the difference between the Akaike information criterion (AIC) of the model with the microclimatic variable and the AIC of a specific reference model without this variable (see following equations); AIC is an indicator of "relative goodness of fit of a statistical model for a given data set" (Akaike, 1974); (4) the variable whose model maximized the difference, i.e. the most explanatory variable, was retained in the second step. Considering the second selection criterion of the Window Pane approach mentioned by Pietravalle et al. (2003), consecutive periods, i.e. same duration but a starting day differing by one day or same starting day but a duration differing by one day should result in similar AIC due to autocorrelations between these

periods. The last selection criterion (Pietravalle et al., 2003) was the similarity of the selected periods between related microclimatic variables such as leaf and air temperatures.

$$NewLesion \sim PastInoculum + MicroclimVar_{TxDy} \quad (binomial\ GLM) \quad (1)$$
$$reference\ model: NewLesion \sim PastInoculum \quad (binomial\ GLM)$$

$$Sporulation \sim LesionAge + MicroclimVar_{TxDy} \quad (binomial\ GLM) \quad (2)$$
$$reference\ model: Sporulation \sim LesionAge \quad (binomial\ GLM)$$

$$InfectiousArea \sim InfectiousArea_{day-7} + MicroclimVar_{TxDy} \quad (gaussian\ GLM) \quad (3)$$
$$reference\ model: InfectiousArea \sim InfectiousArea_{day-7} \quad (gaussian\ GLM)$$

We included a variant in this general method by incorporating in the models some variables that necessarily explain *NewLesion*, *Sporulation* or *InfectiousArea*. Hence, in the models for explaining *NewLesion,* we incorporated a variable called *PastInoculum* (see Eq. 1). This variable represents the averaged inoculum stock available in a specific period before the observation of new coffee leaf rust lesions. This inclusion seemed appropriate as no infection can occur without inoculum. We did not choose an arbitrary period. On the contrary, we used the same method previously described to identify the best past inoculum period to explain *NewLesion* (see Eq. 4). In the models used, we considered the coffee leaf stratum because incidence and severity, and hence quantity of uredospores, have been reported to be higher in the low coffee tree strata (Avelino et al. 1991; Villegas-García and Baeza-Aragón, 1990).

$$NewLesion \sim LeafStratum + Inoculum_{period} \quad (binomial\ GLM) \quad (4)$$
$$reference\ model: NewLesion \sim LeafStratum \quad (binomial\ GLM)$$

329 Similarly, for the sporulation model, the age of the lesion ($LesionAge$) entered in the model
330 since an older lesion has a higher probability of sporulating than a younger one (see Eq. 2). In the
331 last model, for *InfectiousArea* modeling, we included the past infectious area of the lesion (one
332 week before): $InfectiousArea_{\text{day-7}}$ (see Eq. 3). This variable is the lesion infectious area
333 (*InfectiousArea*) measured at the previous monitoring date, so it is a reference for infectious area
334 growth.
335 The second step consisted of building complete generalized linear models (GLMs) for
336 *NewLesion*, *Sporulation* and *InfectiousArea* by including the best microclimatic variables
337 identified in Step One. Only uncorrelated predictors were included in the models. For that
338 purpose, we analyzed the correlation between variables and discarded those with R^2 >0.49
339 (Dormann et al., 2012). We also used biological criteria to finalize certain choices for several
340 variables. The variable *PlantFruitLoad* was included in all of the models for its possible effects
341 on coffee leaf rust development (López-Bravo et al., 2012).
342 Prior to proceeding with the complete model step, the distributions of the selected variables
343 were studied to focus on domains of definition with a sufficient number of observations. When
344 there were interactions between variables, a division into submodels was performed using the
345 "party" package (Hothorn et al., 2006), which builds a tree-based regression by recursive binary
346 partitioning. The binomial models were then evaluated using the package pROC (Robin et al.,
347 2011) that transforms the response variable into a binary response, finding the threshold that
348 maximizes the area under the receiver operating characteristic (ROC) curve. The classification
349 error is then determined by the confusion matrix. We evaluated the Gaussian models by building
350 the regression between observed and predicted data. All statistical analyses were performed with
351 R 3.5.1 (R Development Core Team 2018) and with an alpha level of 0.05. Eqs. 1, 2, 3 and 4 and
352 their reference models (Step One) and complete models (Step Two) were fitted with the GLM

353 function in the lme4 package (Bates et al., 2015). The maximum likelihood of parameters was
354 approximated by the Laplace method (Bolker et al., 2009).
355

356 # 3. Results

357 In the graphs generated in Step One of the analysis, the largest differences in AIC indicate a
358 strong influence of the microclimatic variable averaged on the associated period (Figs. 3, 4, 5, 6).
359 Due to the second selection criteria (Pietravalle et al. 2003) and our approximation of symptom
360 or sign onset by the midpoint of the two monitoring dates, the periods of influence were visible
361 on the graphs by areas of higher AICs rather than punctual dots. Table 3 indicates the selected
362 periods for each microclimatic variable: a starting date for the consideration of the variable (T),
363 in days before foliar site status change, and duration in days (D). Only uncorrelated and
364 significant variables were kept in the models. In the final models equations, we indicated the
365 parameter estimates with Greek letters described in Table 4.
366

367 ## 3.1. Predictive model of the probability of lesion emergence per foliar site

368 By exploring the influence periods of the inoculum stock on *NewLesion*, we were able to
369 identify the best period of influence of *PastInoculum* (Eq. 1): between five and three weeks
370 before the lesion appeared (Fig. 3). From the 26 microclimatic variables resulting from this first
371 selection (Fig. 4), only three uncorrelated variables were conserved and had a significant effect:
372 the average daily rainfall recorded between 33 and 24 days before lesion emergence ($Rain_{T33D10}$),
373 the average daily minimum leaf temperature recorded between 20 and 18 days before lesion
374 emergence ($TcMin_{T20D3}$) and the average daily thermal amplitude of the leaves recorded between

20 and 10 days before lesion emergence ($TcAmp_{T20D11}$). Prior to design of the complete model, we removed the microclimatic data combinations not well-represented in the distributions of these variables (Fig. 7). The final data sets of models A1 and A2 contained 223 945 and 347 491 observations respectively. We found interactions including the average rainfall recorded between 33 and 24 days before lesion emergence ($Rain_{T33D10}$). Because this variable had a unimodal effect, we created two models (A1 and A2) based on two rainfall classes determined by the tree-based regression built by recursive binary partitioning: ≤4 mm per day and >4 mm per day.

$$Model\ A1\ (n = 223945, Rain_{T33D10} \leq 4\,mm): \quad with\ x = \alpha_{1.1} + \alpha_{1.2} \times PastInoculum + \alpha_{1.3} \times Rain_{T33D10} + \alpha_{1.4} \times TcMin_{T20D3} + \alpha_{1.5} \times TcAmp_{T20D11}$$

$$NewLesion = \frac{\exp(x)}{1 + \exp(x)}$$

$$Model\ A2\ (n = 347491, Rain_{T33D10} > 4\,mm): \quad with\ x = \alpha_{2.1} + \alpha_{2.2} \times PastInoculum + \alpha_{2.3} \times Rain_{T33D10} + \alpha_{2.4} \times (Rain_{T33D10})^2 + \alpha_{2.5} \times TcMin_{T20D3} + \alpha_{2.6} \times (TcMin_{T20D3})^2 + \alpha_{2.7} \times TcAmp_{T20D11}$$

$$NewLesion = \frac{\exp(x)}{1 + \exp(x)}$$

In both models, *PastInoculum* showed a positive effect on *NewLesion* ($p < 0.0001$). In model A1, the effect of the $Rain_{T33D10}$ variable was positive ($p < 0.0001$) (Fig. 8A), while its effect was unimodal with a maximum around 10 mm in model A2 ($p < 0.0001$) (Fig. 8B). $TcMin_{T20D3}$ had a positive effect on *NewLesion* in model A1 ($p < 0.0001$) and a unimodal effect with a maximum of

about 19.5°C in model A2 ($p < 0.0001$). $TcAmp_{T20D11}$ negatively affected *NewLesion* in both models ($p < 0.0486$ in model A1 and $p < 0.0001$ in model A2). Predicted values of *NewLesion* as a function of $Rain_{T33D10}$, $TcMin_{T20D3}$, $TcAmp_{T20D11}$ and *PastInoculum* within the range of observed values are presented in Fig. 8 (A1 and A2 graphs). After transformation into binary responses using classification thresholds of 0.0141 for the A1 model and 0.0590 for A2 model, the confusion matrix of models A1 and A2 indicated a classification error of 0.32 and 0.24, respectively. The *PlantFruitLoad* variable was not kept in the complete model because it did not improve the classification error of each of these models. Models A1 and A2 together expressed a root mean square error of 0.032 in predicting the lesion emergence probability, by plot and by date (Fig. 9A).

3.2. Predictive model of sporulation probability of a coffee leaf rust lesion

We selected 23 microclimatic variables associated with a period (Fig. 5), resulting from Step One of our analysis method, as the best predictors of *Sporulation*. Among these variables, only seven were conserved after removing the highly correlated ones (Table 3). The complete model included four main microclimatic variables: the average daily maximum air temperature recorded between 15 and 12 days before lesion sporulation ($TaMax_{T15D4}$), the average daily rainfall recorded between 12 and 11 days before lesion sporulation ($Rain_{T12D2}$), the average daily rainfall recorded between five and three days before lesion sporulation ($Rain_{T5D3}$) and the average daily thermal amplitude of the leaves recorded four days before lesion sporulation ($TcAmp_{T4D1}$), Among the seven variables that influenced *Sporulation*, two variables were related to the pathogen and the host plant: *LesionAge* and *PlantFruitLoad*.

413 $Model\ B\ (n = 51539)$:

414 $$Sporulation = \frac{\exp(x)}{1+\exp(x)} \quad with\ x = \beta_1$$

415 $$+ \beta_2 \times LesionAge + \beta_3 \times (LesionAge)^2$$

416 $$+ \beta_4 \times PlantFruitLoad$$

417 $$+ \beta_5 \times TaMax_{T15D4} + \beta_6 \times (TaMax_{T15D4})^2$$

418 $$+ \beta_7 \times Rain_{T12D2}$$

419 $$+ \beta_8 \times Rain_{T5D3} + \beta_9 \times (Rain_{T5D3})^2$$

420 $$+ \beta_{10} \times TcAmp_{T4D1}$$

421

422 In order to focus on a domain of definition with a sufficient number of observations, we first
423 removed the microclimatic data combinations not well represented in the distributions, as
424 described in Fig. 7 for models A1 and A2. The final data set of model B contained 51 539
425 observations. *LesionAge* was the variable that most influenced *Sporulation* (Model B), with a
426 maximum effect about 15 days before the date of foliar site status change ($p < 0.0001$).
427 *PlantFruitLoad*, which characterizes host phenology, positively influenced *Sporulation* ($p = 0.0005$). The microclimatic variables $TaMax_{T15D4}$ and $Rain_{T5D3}$ showed a significant unimodal
429 effect ($p < 0.0001$) on *Sporulation,* with respective maxima about 28°C and 10 mm (Fig. 8C). In
430 addition, $Rain_{T12D2}$ had a positive effect on *Sporulation* ($p < 0.0001$), while $TcAmp_{T4D1}$ affected it
431 negatively ($p < 0.0001$). Predicted values of *Sporulation* as a function of $TaMax_{T15D4}$, $Rain_{T5D3}$,
432 $Rain_{T12D2}$, $TcAmp_{T4D1}$, *LesionAge* and *PlantFruitLoad*, within the range of observed values, are
433 presented in Fig. 8B. After transformation into binary responses using a classification threshold
434 of 0.140, the classification error computed by the confusion matrix was 0.39 for this model.
435 However, Model B expressed a root mean square error of 0.070 in predicting the sporulation
436 probability, by plot and by date (Fig. 9B).

437

3.3. Model forecasting coffee leaf rust lesion infectious area

For this last model, eight microclimatic variables were selected at the end of Step One (Fig. 6). Of these variables, only three were kept after removing the highly correlated variables and only two had a significant effect in the complete model (Table 3).

$$Model\ C\ (n = 16363): \quad InfectiousArea = +\gamma_1 + \gamma_2 \times InfectiousArea_{day-7} + \gamma_3 \times TaMax_{T5D1} + \gamma_4 \times (TaMax_{T5D1})^2 + \gamma_5 \times TcAmp_{T1D1}$$

InfectiousArea was mainly explained by *InfectiousArea* $_{day\text{-}7}$. $TaMax_{T5D1}$ had a unimodal effect, with a maximum of about 28°C ($p < 0.0001$) (Fig. 8D). *InfectiousArea* was also affected negatively by $TcAmp_{T1D1}$ ($p < 0.0001$). *PlantFruitLoad* had no significant effect. As we did for models A1 and A2, as shown in Fig. 7, we selected domains of definition of $TaMax_{T5D1}$ and $TcAmp_{T1D1}$ in order to include combinations that represented the data well in model C. These definition domains are shown in Fig. 8C. The final data set of model C contained 16 363 observations. Since this model had a Gaussian response, we did not use the confusion matrix. Model C expressed a root mean square error of 0.012 in predicting the lesion infectious area, by plot and by date (Fig. 9C).

4. Discussion

By modeling foliar site status changes, i.e. lesion level changes, we were able to determine, with no assumptions, complex combinations of microclimatic variables that influence several disease processes. In addition, this approach helped us isolate disease growth from the host

462 dynamics, which is not possible when studying synthetic disease descriptors as incidence or
463 severity (Ferrandino, 2008). As already demonstrated by other studies (Bugaud et al., 2015;
464 Carval et al., 2015; Dorey et al., 2016; Leandro-Muñoz et al., 2017), our results show the
465 importance of exploring different periods of influence of microclimatic variables, as these can
466 vary according to the considered variable and their specific effect. Short duration periods, some
467 only days long, have been identified for several microclimatic variables. These would have been
468 masked if we had considered long periods determined in advance. We showed that the periods of
469 influence of microclimatic variables follow on logically according to their specific effect on
470 disease development instead of overlapping (Fig. 10). Not all of the favourable conditions for
471 disease growth need to be met at the same time and during the same period.

472 Our two models on lesion emergence probability incorporated more adjusted microclimatic
473 variables than the empirical models obtained so far. These variables are consistent with the
474 knowledge of the factors affecting the biology of the fungus. Based on the best estimated
475 inoculum predictor for lesion emergence probability — the period from five to three weeks
476 before the lesion emergence — the incubation period would be at least 21 days. In addition, the
477 period from 20 to 18 days before a lesion emergence in which an influence of the minimum leaf
478 temperature was observed could be related to the uredospore germination and penetration.
479 Indeed, germination is stimulated by the previous exposition to low temperatures recorded at
480 night, and the duration of three days could evoke a survival time of the uredospores (Nutman et
481 al., 1963). This hypothesis would imply that the incubation period would be around three weeks,
482 a result in agreement with the findings of Leguizamón-Caycedo et al. (1998), who measured
483 incubation periods ranging from 18 to 24 days depending on the level of shade in their studies on
484 the Caturra coffee variety in Colombia.

485 In our study, the unimodal effect of the average rainfall between 33 to 24 days before lesion
486 emergence could therefore correspond to the dissemination phase of the uredospores. We
487 hypothesize that uredospore release and deposition occur with rainfall below 10 mm, in
488 accordance with previous works (Bock, 1962; Nutman et al., 1960). However, above 10 mm,
489 uredospore wash-off by rain probably occurs, decreasing the probability of lesion emergence.
490 Uredospore wash-off by rain has already been recognized as a strong limitation for *H. vastatrix*
491 propagation (Avelino et al., 2019; Savary et al., 2004) and in other pathosystems (Sache, 2000).
492 Under the conditions of our trial, in agroforestry systems, dispersal is mainly carried out by rain
493 through raindrop impact on leaves, rather than by wind (Boudrot et al., 2016). The presence of
494 trees in agroforestry systems and in the landscape helps intercept wind, limiting its effect
495 (Avelino et al., 2012; Boudrot et al., 2016; Pezzopane et al., 2011). In other conditions, however,
496 wind has been considered as the main factor affecting uredospore dispersal (Becker et al., 1975).
497 Once the uredospore is located on the underside surface of the leaf, where the stomata that
498 serve as entry doors to the fungus are located, uredospore germination, germ tube growth and
499 appressorium formation phases require the presence of water and low light intensity (Rayner
500 1961). In our study, the water required for these phases was not a limiting factor since the leaves
501 were always wet at night because of dew. The last microclimatic variable included in our two
502 models on lesion emergence probability was the average thermal amplitude of the leaves between
503 20 and 10 days before symptom onset. This finding possibly illustrates the influence of leaf
504 temperature on the colonization phase of the fungus (Kushalappa and Eskes, 1989; Ribeiro,
505 1978). The values of the lesion emergence probability are in general low: 75% of the values
506 below a probability of 0.04 (Fig. 9A). However, as we subdivided the coffee leaf into 25 foliar
507 sites for potential lesion emergence, this model calculates a probability of occurrence of a lesion
508 per site and not per leaf. A probability of 0.04 at the foliar site scale represents a probability 25

509 times higher at the leaf scale, therefore a probability equal to one for a leaf to become diseased
510 and express the symptoms.

511 Given the complexity of investigating internal leaf-development phases (McCain and Hennen,
512 1984), most studies have focused on studying the latency period. In the case of coffee leaf rust,
513 this period includes the incubation period and the time required by the pathogen to colonize the
514 leaf and produce its first infectious entities via stomata. In our predictive model on sporulation,
515 the most important variable was the age of the lesion, with an optimal age of 15 days to sporulate
516 (Fig. 8C). Microclimatic variables were secondary. This result indicates that once into the leaf,
517 the pathogen was less dependent on external conditions for its growth and sporulation. The
518 optimal age of a lesion for sporulation is the time that the pathogen requires to colonize the
519 mesophyll sufficiently and to accumulate in the substomatal spaces from which the uredospore
520 precursor cells will be differentiated and released (McCain and Hennen, 1984). This optimal
521 lesion age can also be the time needed to accumulate the necessary nutrients for the development
522 of these cells.

523 Few studies have investigated the microclimatic factors that influence the processes of
524 sporulation and growth of the lesion infectious area independently from the infection phase. We
525 hypothesized that the microclimatic periods that we identified were related with stomata
526 functioning that, in turn, affected the occurrence of the subprocesses of coffee leaf rust
527 sporulation (Guggenheim and Harr, 1978). The positive rainfall influence between 12 and 11
528 days and between five and three days before lesion sporulation can be explained by the opening
529 of the stomata under high humidity conditions (Butler, 1977). Stomata opening facilitates the
530 release of sporogenous cells (Guggenheim and Harr, 1978), with a number of emerging
531 sporogenous cells increased with a larger ostiole opening (McCain and Hennen, 1984). In
532 addition, daily leaf temperature amplitude four days before lesion sporulation negatively affected

533 sporulation, possibly because high temperatures, increasing thermal amplitude, promote stomata
534 closure, due to CO_2 accumulation in the substomatal areas (Heath and Orchard, 1957). Another
535 possible hypothesis is the lethal effect of high temperatures on fungus internal development
536 (Ribeiro, 1978). Finally, the unimodal effect of the daily average of the maximum air
537 temperatures from 15 to 12 days before lesion sporulation, with an optimal temperature around
538 28°C, can be explained by negative effects of low temperatures (Toniutti et al., 2017) and high
539 temperatures on sporulation. This effect could also be related to the colonization phase, as 28°C
540 is the maximum temperature limit for the latent period (Waller, 1982). Finally, the negative part
541 of the unimodal effect of rainfall, from five to three days before lesion sporulation, is not easy to
542 interpret. It can be assumed that days with heavy rainfall will generally be related to lower
543 maximum temperatures, less favorable to sporulation.

544 The last variable included in the sporulation model was the plant fruit load, estimated by the
545 number of fruiting nodes per plant, which was found to have a positive effect on the sporulation
546 probability of the lesions. This result is compatible with the hypothesis of a migration, from
547 leaves to fruits, of phenolic compounds involved in the plant's defense mechanisms (Chalfoun
548 and Carvalho, 1987).

549 Despite these interesting results, our model appeared rather inaccurate since the model
550 explained only 26% of the sporulation probability. This low precision is possibly due to a high
551 variability in leaf temperature within the same coffee layer (Miller, 1971) that our measurements
552 did not capture. Indeed, the radiation received by the leaves can vary greatly, especially in the
553 lower strata, which benefit from the partial and irregular shade provided by the upper stratum of
554 the coffee plants and that of neighboring coffee plants (Butler, 1977). Another hypothesis to
555 explain the inaccuracy could be our consideration of plant fruit load in the model without taking
556 into account the development stage of fruits. Indeed, within fruit development, there is a

557 progressive migration from leaves to fruits of phenolic compounds known for their role in plant
558 defense mechanisms (de Carvalho et al., 2001; Kushalappa and Eskes, 1989).

559 With regard to the model predicting lesion infectious area growth, the variable that logically
560 emerged as the main factor was the past lesion infectious area measured at the last monitoring
561 date. However, this growth was dependent on microclimate variations. Infectious area was larger
562 when maximum air temperature was about 28°C five days before area measurement and leaf
563 temperature amplitude the day before was lower. These short duration effects are probably
564 related to brief phenomena such as stomata opening, releasing more sori. These effects could be
565 similar to those of maximum air temperature and leaf temperature amplitude on sporulation
566 onset.

567 It is important to focus on the predictive potential of the models in terms of time of
568 anticipation. In all of the models we developed, some weather variables had an effect close to the
569 onset of symptoms and signs. In the case of the models predicting the probability of lesion
570 emergence, the earliest influencing variables, the inoculum amount between five and three weeks
571 before lesion emergence and the average rainfall intensity between 30 and 24 days before, can be
572 used to calculate intervals of lesion emergence probability or provide possible scenarios. In
573 contrast, weather does not have an early influence on sporulation and infectious area growth. In
574 these cases, the use of meteorological forecasts with a confidence interval, instead of
575 meteorological measurements, could be used in our models to compute response intervals and
576 suggest possible future scenarios.

577 Our models require monitoring of variables such as the inoculum stock, lesion age and past
578 lesion infectious area. These variables are good predictors, respectively, of infection levels
579 (Kushalappa, 1981), sporulation probability and lesion infectious area and significantly

580 contribute to the accuracy of plant disease prediction models (Krause and Massie, 1975),
581 therefore deserving to be assessed in coffee leaf rust surveillance activities.
582
583 ## 5. Conclusion
584 Our statistical analysis permitted determination, without *a priori* assumptions, of periods of
585 influence per microclimatic variable that vary according to their specific effect on coffee leaf rust
586 development stages instead of hypothetical periods of influence identical for all meteorological
587 variables. This process-based approach, such as mechanistic models, improved our understanding
588 of coffee leaf rust development and enabled building models forecasting the onset of coffee leaf
589 rust symptoms and signs. It is likely that these models can be used in Central American coffee
590 areas with meteorological variables that fit within our domains of definition to predict different
591 risks in terms of coffee leaf rust development stages. These different development stages imply
592 different fungicide type recommendations: protectant fungicides to prevent infection; curative
593 fungicides to suppress colonization and sporulation. However, the accuracy of the sporulation
594 probability model still needs to be improved to consider its application, by incorporating missing
595 variables, as possibly fruit phenology. Due to their simplicity, these models have the advantage
596 that they can be easily evaluated with other datasets and improved. Their use, combined with a
597 crop model in a simulator, could even make it possible to compare the simulated incidences with
598 incidences measured by the monitoring programs of the different Central American countries.
599 The combinations of microclimatic variables that we determined as influencing coffee leaf rust
600 growth also represent valuable information for the development of a mechanistic model. Finally,
601 it would be important to study how agroforestry systems and their management can help regulate

602 coffee leaf rust by modifying potential favourable microclimate conditions to this disease in the
603 understory.
604

605 ## Acknowledgements

606 For their valuable technical work, we thank Alejandra Barquero, Hugo Mendez and Steven
607 Cerdas. This work was developed as part of the "Programa Centroamericano de Gestión Integral
608 de la Roya del Café" (PROCAGICA) funded by the EU (DCI-ALA/2015/365-17). We thank the
609 Ernesto Illy Foundation and CIRAD (Centre de Coopération Internationale en Recherche
610 Agronomique pour le Développement) for their financial support, CATIE, ICAFE and the coffee
611 grower Enrique Montenegro for allowing access to their coffee-based agroforestry systems, and
612 R.Scheck for reviewing the English.

References

Alfonsi, R.R., Ortolani, A.A., Pinto, H.S., Pedro Junior, M.J., Brunini, O., 1974. Associação entre nivel de infecção da ferrugem do cafeeiro, variáveis climáticas e área foliar, observadas em *Coffea arabica*, in: Congresso Brasileiro Sobre Pesquisas Cafeeiras. pp. 80–83.

Almeida, R.P.P., 2018. Emerging plant disease epidemics: Biological research is key but not enough. PLOS Biol 16, e2007020. https://doi.org/10.1371/journal.pbio.2007020

Akaike, H., 1973. Information theory and an extension of the maximum likelihood principle, in: Petrov, B.N., Csáki, F. (Eds.), 2nd International Symposium on Information Theory. Tsahkadsor, Armenia, USSR, Budapest: Akadémiai Kiadó, 267–281.

Avelino, J., Badaroux, J., Boudrot, A., Brenes Loaiza, M.A., Granados, E., Henrion, M., Lopez, D., Merle, I., Pico Rosado, J.T., Segura, B., Vilchez Mendoza, S.J., Smith, M., De Melo, E., 2019. Shade effects on coffee rust (*Hemileia vastatrix*). In: Dupraz Christian, G.M., Lawson Gerry (Ed.), Proceedings of the 4th World Congress on Agroforestry. Book of abstracts, 05-20/05-22 2019, Montpellier, France.

Avelino, J., Cristancho, M., Georgiou, S., Imbach, P., Aguilar, L., Bornemann, G., Läderach, P., Anzueto, F., Hruska, A.J., Morales, C., 2015. The coffee rust crises in Colombia and Central America (2008–2013): impacts, plausible causes and proposed solutions. Food Secur. 7, 303–321. https://doi.org/10.1007/s12571-015-0446-9

Avelino, J., Romero-Gurdián, A., Cruz-Cuellar, H.F., Declerck, F.A., 2012. Landscape context and scale differentially impact coffee leaf rust, coffee berry borer, and coffee root-knot nematodes. Ecol. Appl. 22, 584–596.

Avelino, J., Zelaya, H., Merlo, A., Pineda, A., Ordoñez, M., Savary, S., 2006. The intensity of a coffee rust epidemic is dependent on production situations. Ecol. Model. 197, 431–447. https://doi.org/10.1016/j.ecolmodel.2006.03.013

Avelino, J., Muller, R.A., Cilas, C., Velasco Pascual, H., 1991. Development and behavior of coffee orange rust (*Hemileia vastatrix* Berk. and Br.) in plantations undergoing modernization, planted with dwarf varieties in South-East Mexico. Café Cacao Thé. 35(1), 21-37.

Bates, D., Mächler, M., Bolker, B., Walker, S., 2015. Fitting Linear Mixed-Effects Models Using lme4. J. Stat. Soft. 67. https://doi.org/10.18637/jss.v067.i01

Bebber, D.P., Castillo, Á.D., Gurr, S.J., 2016. Modelling coffee leaf rust risk in Colombia with climate reanalysis data. Philos. Tans. R. Soc. B 371, 20150458. https://doi.org/10.1098/rstb.2015.0458

Becker, S., Mulinge, S.K., Kranz, J., 1975. Evidence that uredospores of *Hemileia vastatrix* Berk. and Br. are wind-borne. Phytopathol. Z. 82, 359-360.

Bock, K.R., 1962. Dispersal of uredospores of *Hemileia vastatrix* under field conditions. Trans. Brit. Mycol. Soc. 45, 63–74. https://doi.org/10.1016/S0007-1536(62)80035-7

Bolker, B.M., Brooks, M.E., Clark, C.J., Geange, S.W., Poulsen, J.R., Stevens, M.H.H., White, J.-S.S., 2009. Generalized linear mixed models: a practical guide for ecology and evolution. Trends Ecol. Evol. 24, 127–135. https://doi.org/10.1016/j.tree.2008.10.008

Boudrot, A., Pico, J., Merle, I., Granados, E., Vílchez, S., Tixier, P., Filho, E. de M.V., Casanoves, F., Tapia, A., Allinne, C., Rice, R.A., Avelino, J., 2016. Shade Effects on the Dispersal of Airborne *Hemileia vastatrix* Uredospores. Phytopathology 106, 572–580. https://doi.org/10.1094/PHYTO-02-15-0058-R

Bugaud, C., Joannès-Dumec, C., Louisor, J., Tixier, P., Salmon, F., 2015. Preharvest temperature affects chilling injury in dessert bananas during storage: Preharvest temperature affects chilling injury in dessert bananas during storage. J. Sci. Food Agric. 96, 2384–2390. https://doi.org/10.1002/jsfa.7354

Butler, D.R., 1977. Coffee Leaf Temperatures in a Tropical Environment. Acta Bot. Neerl. 26, 129–140. https://doi.org/10.1111/j.1438-8677.1977.tb01106.x

Carval, D., Cotté, V., Notaro, M., Ryckewaert, P., Tixier, P., 2015. Spatiotemporal population dynamics of the banana rind thrips, *Elixothrips brevisetis* (Bagnall) (Thysanoptera: Thripidae). J. Appl. Entomol. 139, 510–518. https://doi.org/10.1111/jen.12190

Cerda, R., Avelino, J., Gary, C., Tixier, P., Lechevallier, E., Allinne, C., 2017. Primary and secondary yield losses caused by pests and diseases: Assessment and modeling in coffee. PLOS ONE 12, e0169133.

Chalfoun, S.M., de Carvalho, V.D., 1987. Efeito da produçao e da composiçao química de folhas de cafeeiros sobre a intensidade de ataque de ferrugem (*Hemileia vastatrix* Berk & Br.), in: 14° Congresso Brasileiro de Pesquisas Cafeeiras, 1° Congresso Latinoamericano de Tecnologia Cafeeira, Ministerio da Indústria e do Comercio, Instituto Brasileiro do Café: Campinas 121-122.

Cintra, M.E., Meira, C.A.A., Monard, M.C., Camargo, H.A., Rodrigues, L.H.A., 2011. The use of fuzzy decision trees for coffee rust warning in Brazilian crops, in: 2011 11th International Conference on Intelligent Systems Design and Applications. IEEE, Cordoba, Spain, pp. 1347–1352. https://doi.org/10.1109/ISDA.2011.6121847

Coakley, S.M., Line, R.F., 1982. Prediction of stripe rust epidemics on winter wheat using statistical models. Phytopathology 72, 1006.

Corrales, D.C., Casas, A.F., Ledezma, A., Corrales, J.C., 2016. Two-Level Classifier Ensembles for Coffee Rust Estimation in Colombian Crops: International Journal of Agricultural and Environmental Information Systems 7, 41–59. https://doi.org/10.4018/IJAEIS.2016070103

Corrales, D.C., Figueroa, A., Ledezma, A., Corrales, J.C., 2015. An Empirical Multi-classifier for Coffee Rust Detection in Colombian Crops, in: Gervasi, O., Murgante, B., Misra, S., Gavrilova, M.L., Rocha, A.M.A.C., Torre, C., Taniar, D., Apduhan, B.O. (Eds.), Computational Science and Its Applications -- ICCSA 2015. Springer International Publishing, Cham, pp. 60–74. https://doi.org/10.1007/978-3-319-21404-7_5

Cunniffe, N.J., Koskella, B., E. Metcalf, C.J., Parnell, S., Gottwald, T.R., Gilligan, C.A., 2015. Thirteen challenges in modelling plant diseases. Epidemics 10, 6–10. https://doi.org/10.1016/j.epidem.2014.06.002

de Carvalho, V.L., Chalfoun, S.M., Castro, H.A., de Carvalho, V.D., 2001. Influência de diferentes níveis de produção sobre a evolução da ferrugem do cafeeiro e sobre teores foliares de compostos fenólicos. Ciênc. agrotec. 25, 49–54.

de Moraes, S.A., Sugimori, M.H., Ribeiro, I.J.A., Ortolani, A.A., Pedro Jr., M.J., 1976. Incubation period of *Hemileia vastatrix* B. et Br. in three regions of Sao Paulo State. Summa Phytopathol. 2, 32–38.

de Wolf, E.D., Isard, S.A., 2007. Disease Cycle Approach to Plant Disease Prediction. Annu. Rev. Phytopathol. 45, 203–220. https://doi.org/10.1146/annurev.phyto.44.070505.143329

Dorey, E., Fournier, P., Léchaudel, M., Tixier, P., 2016. A statistical model to predict titratable acidity of pineapple during fruit developing period responding to climatic variables. Scientia Horticulturae 210, 19–24. https://doi.org/10.1016/j.scienta.2016.07.014

Dormann, C.F., Elith, J., Bacher, S., Buchmann, C., Carl, G., Carré, G., Garcia Marquéz, J.R., Gruber, B., Lafourcade, B., Leitão, P.J., Münkemüller, T., McClean, C., Osborne, P.E., Reineking, B., Schröder, B., Skidmore, A.K., Zurell, D., Lautenbach, S., 2012. Collinearity: a review of methods to deal with it and a simulation study evaluating their performance. Ecography 35, 1–20.

Eskes, A.B., De Souza, E.Z., 1981. Ataque da ferrugem em ramos com e sem produçao, de plantas do cultivar catuaí. In: Congresso Brasileiro de Pesquisas Cafeeiras, Sao Lourenzo, Minas Gerais, (Brasil) : IBC, 186-8.

Ferrandino, F.J., 2008. Effect of Crop Growth and Canopy Filtration on the Dynamics of Plant Disease Epidemics Spread by Aerially Dispersed Spores. Phytopathology 98, 492–503. https://doi.org/10.1094/PHYTO-98-5-0492

Guggenheim, R., Harr, J., 1978. Contributions to the Biology of *Hemileia vastatrix* II. SEM-Investigations on Sporulation of *Hemileia vastatrix* on Leaf Surfaces of *Coffea arabica*. J. Phytopathol. 92, 97–101. https://doi.org/10.1111/j.1439-0434.1978.tb03590.x

Jha, S., Bacon, C.M., Philpott, S.M., Ernesto Méndez, V., Läderach, P., Rice, R.A. 2014. Shade Coffee: Update on a Disappearing Refuge for Biodiversity. BioScience. 64, 416–428.

Heath, O.V.S., Orchard, B., 1957. Midday closure of stomata. Temperature effects on the minimum intercellular space carbon dioxide concentration "I". Nature 180, 180-181.

Hinnah, F.D., Sentelhas, P.C., Meira, C.A.A., Paiva, R.N., 2018. Weather-based coffee leaf rust apparent infection rate modeling. Int. J. Biometeorol. 62, 1847–1860. https://doi.org/10.1007/s00484-018-1587-2

Holguín, F., 1987. Estudios epidemiológicos de la roya del cafeto en México, in: X Simposio Latinoamericano sobre Caficultura, IICA: Tapachula, Chiapas, (México). 32-39.

Hothorn, T., Hornik, K., Zeileis, A., 2006. Unbiased Recursive Partitioning: A Conditional Inference Framework. J. Comput. Graph. Stat. 15, 651–674. https://doi.org/10.1198/106186006X133933

Krause, R.A., Massie, L.B., 1975. Predictive Systems: Modern Approaches to Disease Control. Annu. Rev. Phytopathol. 13, 31–47. https://doi.org/10.1146/annurev.py.13.090175.000335

Kushalappa, A.C., Chaves, G.M., 1980. An analysis of the development of coffee rust in the field. Fitopatol. Bras. 5, 95-103

Kushalappa, A.C., Martins, C.P., 1980. Incubation and generation periods for *Hemileia vastatrix* on coffee in Viçosa, Minas Gerais. Fitopatol. Bras. 5, 177-183

Kushalappa, A.C., 1981. Linear Models Applied to Variation in the Rate of Coffee Rust Development. J. Phytopathol. 101, 22–30. https://doi.org/10.1111/j.1439-0434.1981.tb03317.x

Kushalappa, A.C., Akutsu, M., Ludwig, A., 1983. Application of Survival Ratio for Monocyclic Process of *Hemileia vastatrix* in Predicting Coffee Rust Infection Rates. Phytopathology 73, 96–103. https://doi.org/10.1094/Phyto-73-96

Kushalappa, A.C., Akutsu, M., Oseguera, S.H., Chaves, G.M., Melles, C.A., Miranda, J.M., Bartolo, G.F., 1984. Equations for predicting the rate of coffee rust development based on net survival ratio for macrocyclic process of *Hemileia vastatrix*. Fitopatol. Bras. 9, 255-271.

Kushalappa, A.C., Hernández, T.A., Lemos, H.G., 1986. Evaluation of simple and complex coffee rust forecasts to time fungicide application. Fitopatol. Bras. 11, 515-526.

Kushalappa, A.C., Eskes, A.B., 1989. Advances in Coffee Rust Research. Annu. Rev. Phytopathol. 27, 503–531.

740 Lin, B.B., 2007. Agroforestry management as an adaptive strategy against potential microclimate
741 extremes in coffee agriculture. Agric. Forest Meteorol. 144, 85–94.

742 Leandro-Muñoz, M.E., Tixier, P., Germon, A., Rakotobe, V., Phillips-Mora, W., Maximova, S., Avelino,
743 J., 2017. Effects of microclimatic variables on the symptoms and signs onset of *Moniliophthora*
744 *roreri*, causal agent of Moniliophthora pod rot in cacao. PLOS ONE 12, e0184638.
745 https://doi.org/10.1371/journal.pone.0184638

746 Leguizamón-Caycedo, J., Orozco-Gallego, L., Gómez-Gómez, L., 1998. Períodos de incubación (PI) y de
747 latencia (PL) de la roya del cafeto en la zona central cafetera de Colombia. Cenicafé 49, 325–339.

748 Liebig, T., Ribeyre, F., Läderach, P., Poehling, H.-M., van Asten, P., Avelino, J., 2019. Interactive effects
749 of altitude, microclimate and shading system on coffee leaf rust. J. Plant Interact. 14, 407–415.
750 https://doi.org/10.1080/17429145.2019.1643934

751 López-Bravo, D.F., Virginio-Filho, E. de M., Avelino, J., 2012. Shade is conducive to coffee rust as
752 compared to full sun exposure under standardized fruit load conditions. Crop Prot. 38, 21–29.
753 https://doi.org/10.1016/j.cropro.2012.03.011

754 Luaces, O., Rodrigues, L.H.A., Meira, C.A.A., Quevedo, J.R., Bahamonde, A., 2010. Viability of an
755 alarm predictor for coffee rust disease using interval regression, in: International Conference on
756 Industrial, Engineering and Other Applications of Applied Intelligent Systems. Springer, pp. 337–
757 346.

758 McCain, J.W., Hennen, J.F., 1984. Development of the uredinial thallus and sorus in the orange rust
759 fungus, *Hemileia vastatrix*. Phytopathology 74, 714-721.

760 Meira, C.A., Rodrigues, L.H., Moraes, S.A., 2008. Análise Da Epidemia Da Ferrugem Do Cafeeiro Com
761 árvore De Decisão. Trop. Plant Pathol. 33, 114–124.

762 Meira, C.A.A., Rodrigues, L.H.A., Moraes, S.A. de, 2009. Modelos de alerta para o controle da ferrugem-
763 do-cafeeiro em lavouras com alta carga pendente. Pesq. agropec. bras. 44, 233–242.

764 Merle, I., Pico, J., Granados, E., Boudrot, A., Tixier, P., Virginio Filho, E.M., Cilas, C., Avelino, J., 2019.
765 Unraveling the complexity of coffee leaf rust behavior and development in different *Coffea*
766 *arabica* agro-ecosystems. Phytopathology. In press.

767 Miller, P.C., 1971. Sampling to Estimate Mean Leaf Temperatures and Transpiration Rates in Vegetation
768 Canopies. Ecology 52, 885–889. https://doi.org/10.2307/1936038

769 Nutman, F.J., Roberts, F.M., Bock, K.R., 1960. Method of uredospore dispersal of the coffee leaf-rust
770 fungus, *Hemileia vastatrix*. Trans. Brit. Mycol. Soc. 43, 509-IN6. https://doi.org/10.1016/S0007-
771 1536(60)80033-2

772 Nutman, F.J., Roberts, F.M., Clarke, R.T., 1963. Studies on the biology of *Hemileia vastatrix* Berk. & Br.
773 Trans. Brit. Mycol. Soc. 46, 27–44. https://doi.org/10.1016/S0007-1536(63)80005-4

774 Pedro, M.J., 1983. Effects of Meteorological Factors on the Development of Coffee Leaf Rust. EPPO
775 Bull. 13, 153–155. https://doi.org/10.1111/j.1365-2338.1983.tb01592.x

776 Perez-Ariza, C.B., Nicholson, A.E., Flores, M.J., 2012. Prediction of coffee rust disease using bayesian
777 networks, in: Sixth European Workshop on Probabilistic Graphical Models. Granada (Spain), pp.
778 259–266.

779 Pezzopane, J.R.M., Souza, P.S. de, Rolim, G.D.S., Gallo, P.B., 2011. Microclimate in coffee plantation
780 grown under grevillea trees shading. Acta Sci. Agron. 33, 201–206.
781 https://doi.org/10.4025/actasciagron.v33i2.7065

Pietravalle, S., Shaw, M.W., Parker, S.R., van den Bosch, F., 2003. Modeling of relationships between weather and Septoria tritici epidemics on winter wheat: A critical approach. Phytopathology 93,1329-1339.

Pinto, A.C.S., Pozza, E.A., de Souza, P.E., Pozza, A.A.A., Talamini, V., Boldini, J.M., Santos, F.S., 2002. Description of epidemics of coffee rust with neural networks. Fitopatol. Bras. 27, 517–524. https://doi.org/10.1590/S0100-41582002000500013

Rayner, R.W., 1961. Germination and penetration studies on coffee rust (*Hemileia vastatrix* B. & Br.). Annals of Applied Biology 49, 497–505. https://doi.org/10.1111/j.1744-7348.1961.tb03641.x

Ribeiro, I.J.A., 1978. Efeito de alta temperatura no desenvolvimento de *Hemileia vastatrix* em cafeeiro suscetível. Bragantia 37, 11–16.

Robin, X., Turck, N., Hainard, A., Tiberti, N., Lisacek, F., Sanchez, J.-C., Müller, M., 2011. pROC: an open-source package for R and S+ to analyze and compare ROC curves. BMC Bioinformatics 12, 77. https://doi.org/10.1186/1471-2105-12-77

Rudin, C., 2019. Stop explaining black box machine learning models for high stakes decisions and use interpretable models instead. Nature Machine Intelligence 1, 5, 206.

Sache, I., 2000. Short-distance dispersal of wheat rust spores by wind and rain. Agronomie 20, 757–767.

Santacreo, R., Polanco, E., Oseguera, S., 1983. Periodo de incubación y generación de *Hemileia vastatrix* Berk. & Br. en tres zonas cafetaleras de Honduras, Centro América, in: VI Simposio Latinoamericano sobre Caficultura, IICA: Panamá (Panamá). 109-127.

Savary, S., Janeau, J.L., Allorent, D., Escalante, M, Avelino, J., Willocquet, L., 2004. Effects of simulated rainfall events on spore dispersal and spore stocks in three tropical pathosystems. Phytopathology 94:S92

Schindelin, J., Rueden, C.T., Hiner, M.C., Eliceiri, K.W., 2015. The ImageJ ecosystem: An open platform for biomedical image analysis: THE IMAGEJ ECOSYSTEM. Mol. Reprod. Dev. 82, 518–529. https://doi.org/10.1002/mrd.22489

Siettos, C.I., Russo, L., 2013. Mathematical modeling of infectious disease dynamics. Virulence 4, 295–306. https://doi.org/10.4161/viru.24041

Toniutti, L., Breitler, J.-C., Etienne, H., Campa, C., Doulbeau, S., Urban, L., Lambot, C., Pinilla, J.-C.H., Bertrand, B., 2017. Influence of Environmental Conditions and Genetic Background of Arabica Coffee (*C. arabica* L) on Leaf Rust (*Hemileia vastatrix*) Pathogenesis. Front. Plant Sci. 8. https://doi.org/10.3389/fpls.2017.02025

Tronconi, N., Palma, M.R., Suazo, G., Zaldívar, R., Agurcia, R.D., 1995. Periodo de incubación y generación de *Hemileia vastatrix* Berk & Br. en Honduras, in: V Seminario Nacional de Investigación y de Transferencia en Caficultura, IHCAFE: Tegucigalpa (Honduras). 165-173.

Villegas-García, C., Baeza-Aragón, C.A., 1990. Diseminación de *Hemileia vastatrix* Berk. y Br. a nivel del árbol, en un foco natural. Cenicafé 41, 39–49.

Waller, J.M., 1982. Coffee rust-epidemiology and control. Crop Prot. 1, 385–404. https://doi.org/10.1016/0261-2194(82)90022-9

Titles for figures

822 **Fig. 1.** Symptoms and signs of *Hemileia vastatrix* on the under-side of a coffee leaf. Photographs
823 by Steven Cerdas Hernandez taken in Turrialba the 7th, the 14th and 28th of June 2017
824 from left to right.

825 **Fig. 2.** Graphics showing daily rainfall (black bar plot) and daily minimum (blue points) and
826 maximum (orange points) air temperatures measured by the weather stations in the four
827 plots from May 2017 to July 2018. In Turrialba, for both coffee plots in full sun and under
828 medium shade, there was only one rain gauge, set in the full sun coffee plot.

829 **Fig. 3.** Inoculum stock influence on lesion emergence probability, per periods from one to eight
830 weeks before the symptom detection (abscises) and for durations from one to eight weeks
831 (ordinates). The scale on the right indicates the absolute difference between Akaike
832 information criterion (AIC) of the model including the inoculum stock averaged over the
833 considered periods (dates and durations) (*NewLesion ~ LeafStratum + Inoculum* $_{period}$) and
834 AIC of its reference model without including the inoculum stock (*NewLesion ~*
835 *LeafStratum*). The highest AIC difference, labelled with a white square, indicates the period
836 to be considered for inoculum stock that better explains the lesion emergence probability: 5
837 weeks before lesion emergence for 3 weeks. Code explanations are available in Table 2.

838 **Fig. 4.** Influence of microclimatic variables on lesion emergence probability by foliar site, per
839 periods from one to 40 days before the symptom detection (abscises) and for durations from
840 one to 40 days (ordinates). The scale on the right indicates the absolute difference between
841 Akaike information criterion (AIC) of the model including the microclimatic variable
842 averaged over the considered periods (dates and durations) (*NewLesions ~ PastInoculum +*
843 *MicroclimVar* $_{period}$) and AIC of its reference model without including the microclimatic
844 variable (*NewLesions ~ PastInoculum*). The highest AIC differences, labelled with black
845 circles, indicate the periods, to be considered for the microclimatic variable, that better
846 explain the lesion emergence probability.

847 **Fig. 5.** Influence of microclimatic variables on sporulation probability, per periods from one to 28
848 days before the sign detection (abscises) and for durations from one to 28 days (ordinates).
849 The scale on the right indicates the absolute difference between Akaike information
850 criterion (AIC) of the model including the microclimatic variable averaged over the
851 considered periods (dates and durations) (*Sporulation ~ LesionAge + MicroclimVar* $_{period}$)

and AIC of its reference model without including the microclimatic variable (*Sporulation ~ LesionAge*). The highest AIC differences, labelled with black circles, indicate the periods, to be considered for the microclimatic variable, that better explain sporulation probability.

Fig. 6. Influence of microclimatic variables on lesion infectious area growth, per periods from one to seven days before the lesion infectious area growth (abscises) and for durations from one to seven days (ordinates). The scale on the right indicates the absolute difference between Akaike information criterion (AIC) of the model including the microclimatic variable averaged over the considered periods (dates and durations) (*InfectiousArea ~ InfectiousArea* $_{day\text{-}7}$ *+ MicroclimVar* $_{period}$) and AIC of its reference model without including the microclimatic variable (*InfectiousArea ~ InfectiousArea* $_{day\text{-}7}$). The highest AIC differences, labelled with black circles, indicate the periods, to be considered for the microclimatic variable, that better explain lesion infectious area growth.

Fig. 7. Graphs displaying the distributions of the microclimatic variables used to develop the complete model forecasting the lesion emergence probability by foliar site. Grey areas are removed ranges due to under representation of data. $TcMin_{T20D3}$: averaged daily minimum leaf temperature over a period of three days starting 20 days before lesion emergence; $Rain_{T33D10}$: averaged daily rainfall over a period of 10 days starting 33 days before lesion emergence; $TcAmp_{T20D11}$: averaged daily amplitude of leaf temperature over a period of 11 days starting 20 days before lesion emergence.

Fig. 8. Predictions of models A1 and A2 (graphs A1 and A2) for the lesion emergence probability of one of the 25 leaf sites considered, model B for sporulation probability (graph B) and model C for lesion infectious area growth (graph C). Graphs A1 and A2 were presented among model's variation ranges of $Rain_{T33D10}$ and $TcMin_{T20D3}$, while $TcAmp_{T20D11}$ (ranges [6.2:17.9] in model A1 and [7.1:17.3] in model A2) was fixed to its mean and *PastInoculum* (range [0:1.1] in model A1 and [0:3.8] in model A2) to its first (clear grey) and third quantiles (dark grey). Graph B was represented among variation ranges of $TaMin_{T15D4}$ and $Rain_{T5D3}$, while $Rain_{T12D2}$ (range [0:28.3]), $TcAmp_{T4D1}$ (range [5.9:18.9]) and *PlantFruitLoad* (range [0:1150]) were fixed to their mean and *LesionAge* (range [0:50]) was fixed to seven (clear grey), fifteen (grey) and 23 days (dark grey). Graph C was presented among variation ranges of $TaMax_{T5D1}$ and $TcAmp_{T1D1}$ and *InfectiousArea* $_{day\text{-}7}$

(range [0:0.295]) was fixed to its first (clear grey) and third quantiles (dark grey). All the variables are described in Tables 2 and 4.

Fig. 9. Regressions between predicted values and observed averaged values by plot and date for new lesion emergence probability by foliar site (A), sporulation probability (B) and lesion infectious area (C).

Fig. 10. Representations with a time axis of the variables corresponding to the complete models A1, A2, B and C. The box color of the variables indicates a positive effect (white), a negative effect (black) and a unimodal effect with a maximum (grey).

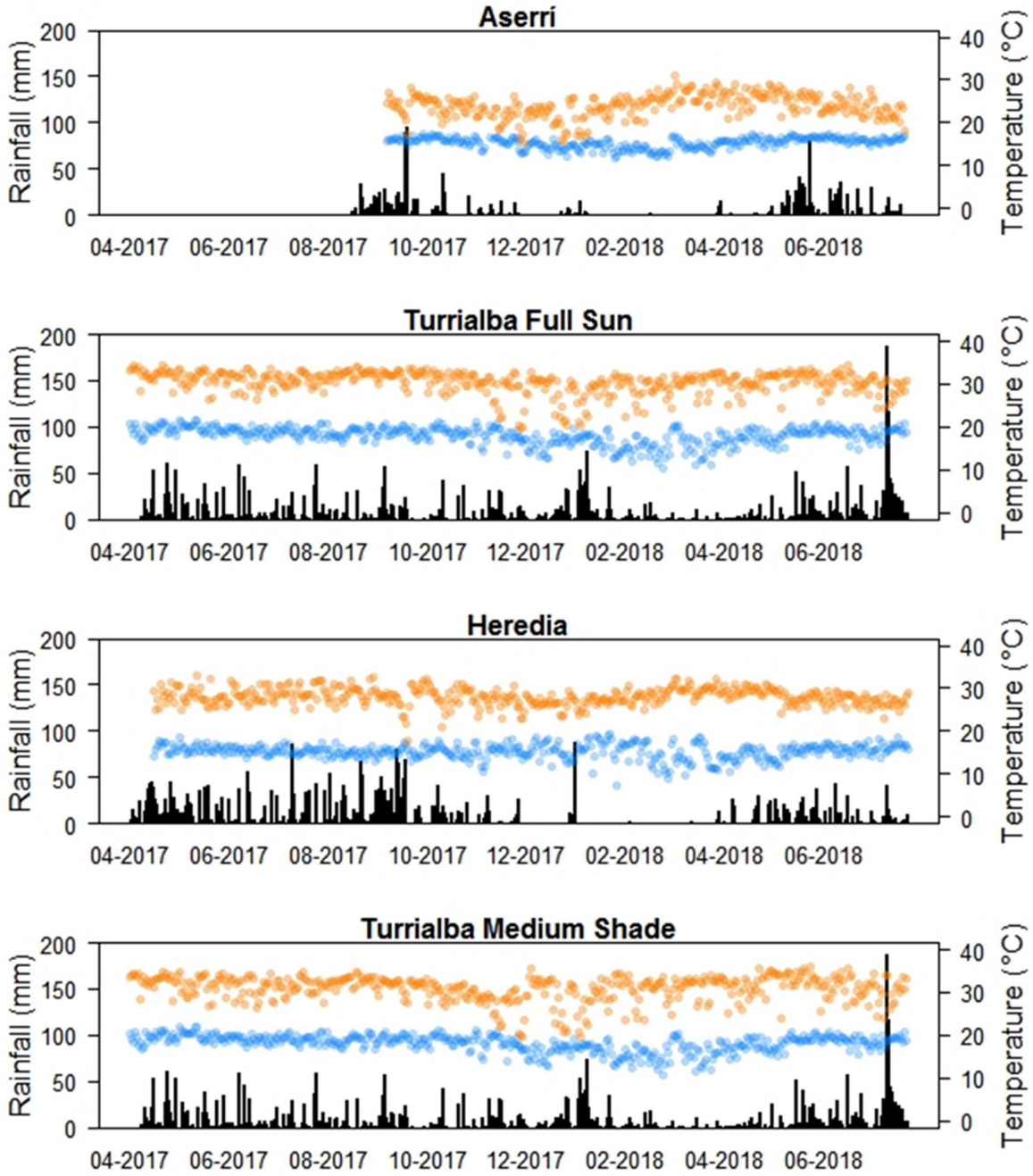

Fig. 1. Graphics showing daily rainfall (black bar plot) and daily minimum (blue points) and maximum (orange points) air temperatures measured by the weather stations in the four plots from May 2017 to July 2018. In Turrialba, for both coffee plots in full sun and under medium shade, there was only one rain gauge, set in the full sun coffee plot.

Fig. 2. Symptoms and signs of *Hemileia vastatrix* on the under-side of a coffee leaf. Photographs by Steven Cerdas Hernandez taken in Turrialba the 7th, the 14th and 28th of June 2017 from left to right.

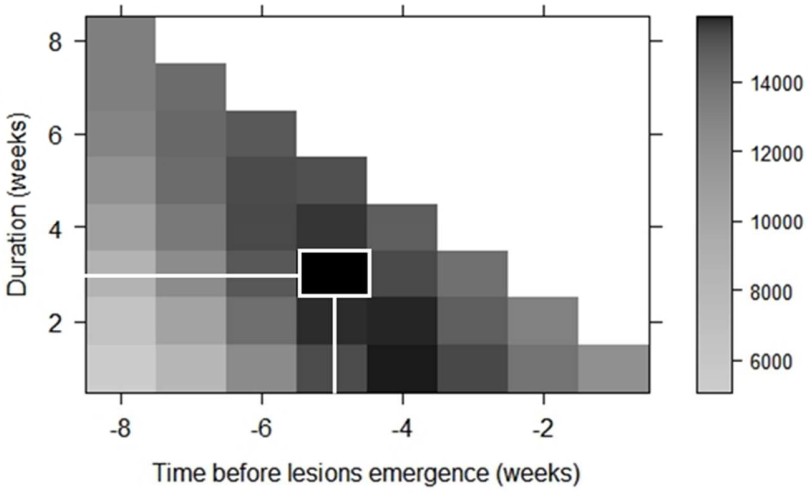

Fig. 3. Inoculum stock influence on lesion emergence probability, per periods from one to eight weeks before the symptom detection (abscises) and for durations from one to eight weeks (ordinates). The scale on the right indicates the absolute difference between Akaike information criterion (AIC) of the model including the inoculum stock averaged over the considered periods (dates and durations) (*NewLesion ~ LeafStratum + Inoculum* $_{period}$) and AIC of its reference model without including the inoculum stock (*NewLesion ~ LeafStratum*). The highest AIC difference, labelled with a white square, indicates the period to be considered for inoculum stock that better explains the lesion emergence probability: 5 weeks before lesion emergence for 3 weeks. Code explanations are available in Table 2.

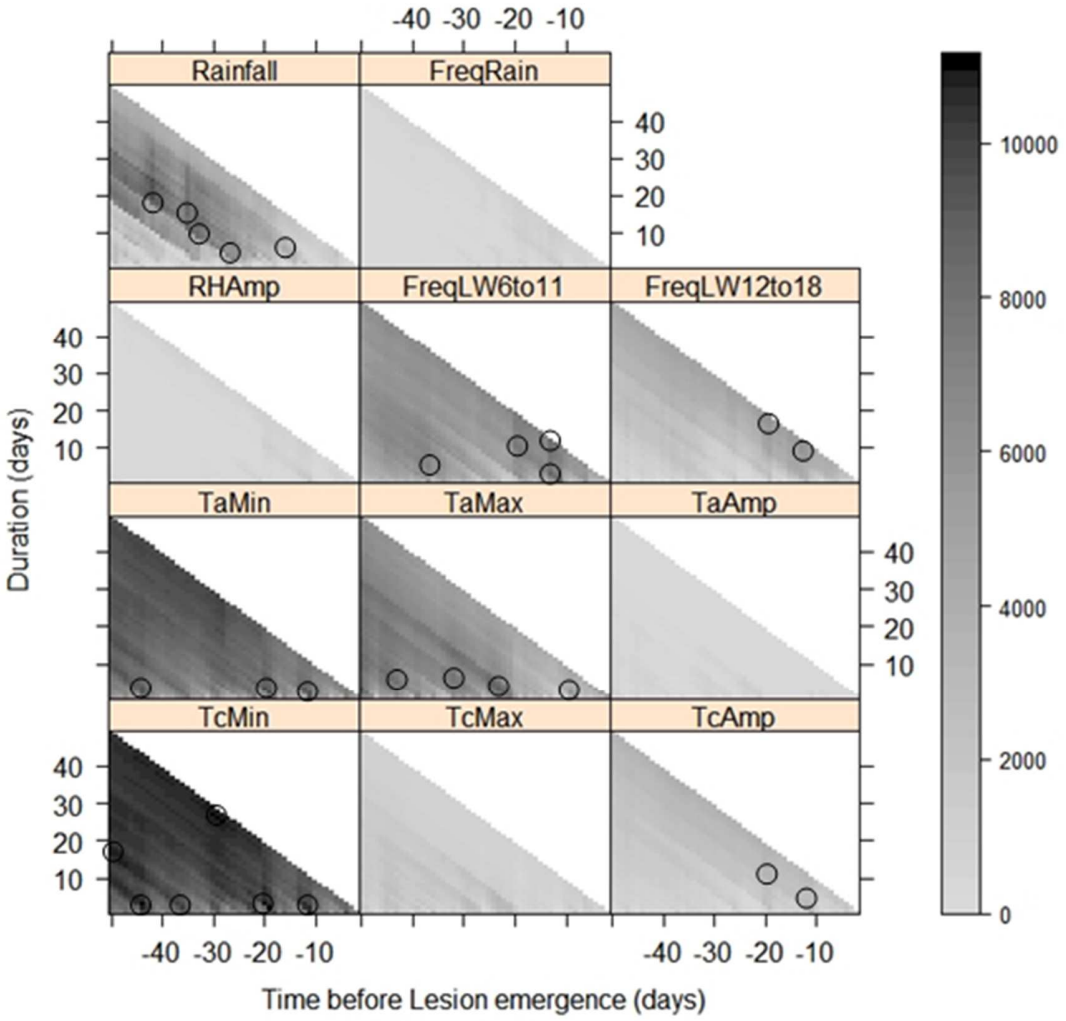

Fig. 4. Influence of microclimatic variables on lesion emergence probability by foliar site, per periods from one to 50 days before the symptom detection (abscises) and for durations from one to 50 days (ordinates). The scale on the right indicates the absolute difference between Akaike information criterion (AIC) of the model including the microclimatic variable averaged over the considered periods (dates and durations) (*NewLesions ~ PastInoculum + MicroclimVar* $_{period}$) and AIC of its reference model without including the microclimatic variable (*NewLesions ~ PastInoculum*). The highest AIC differences, labelled with black circles, indicate the periods, to be considered for the microclimatic variable, that better explain the lesion emergence probability.

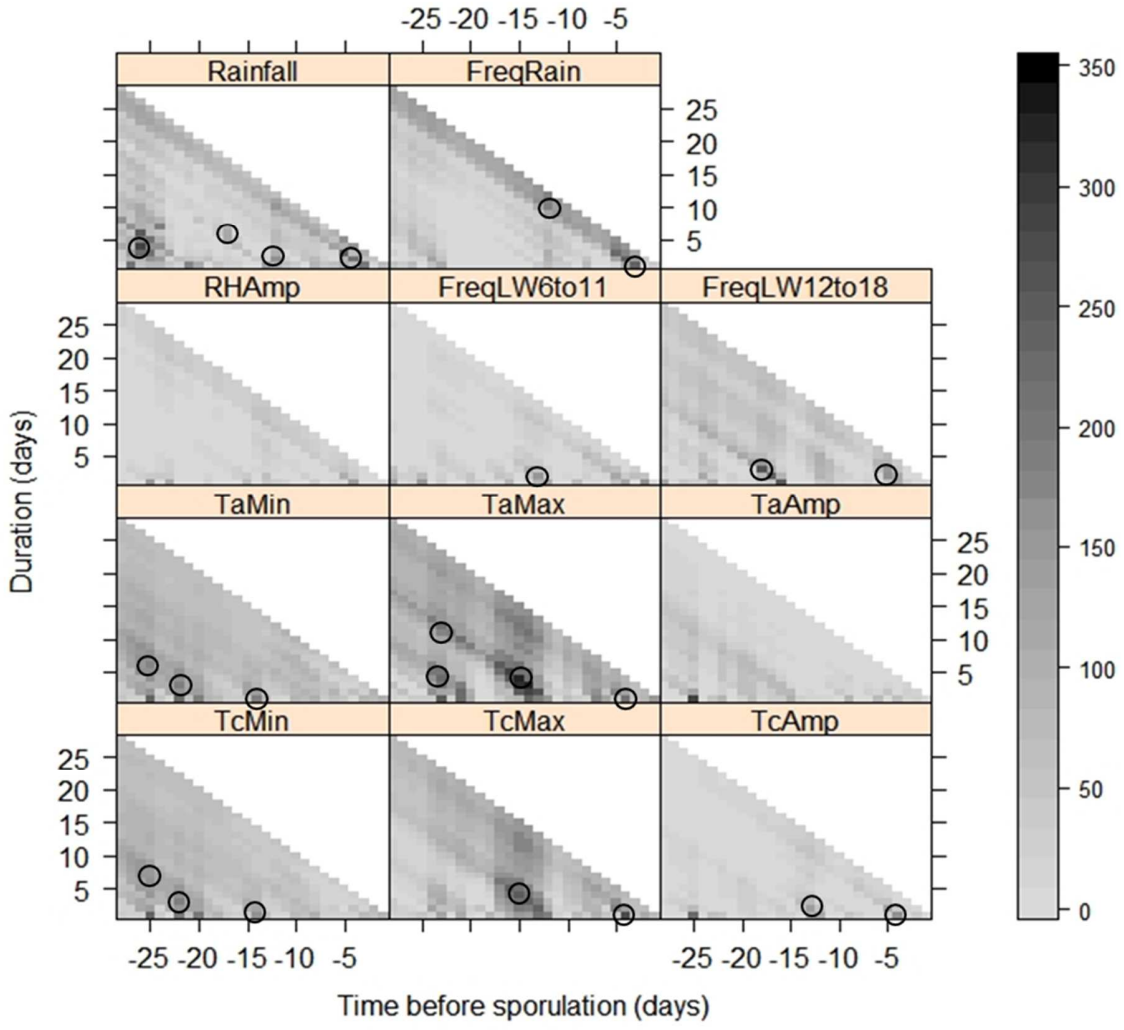

Fig. 5. Influence of microclimatic variables on sporulation probability, per periods from one to 28 days before the sign detection (abscises) and for durations from one to 28 days (ordinates). The scale on the right indicates the absolute difference between Akaike information criterion (AIC) of the model including the microclimatic variable averaged over the considered periods (dates and durations) (*Sporulation ~ LesionAge + MicroclimVar* $_{period}$) and AIC of its reference model without including the microclimatic variable (*Sporulation ~ LesionAge*). The highest AIC differences, labelled with black circles, indicate the periods, to be considered for the microclimatic variable, that better explain sporulation probability.

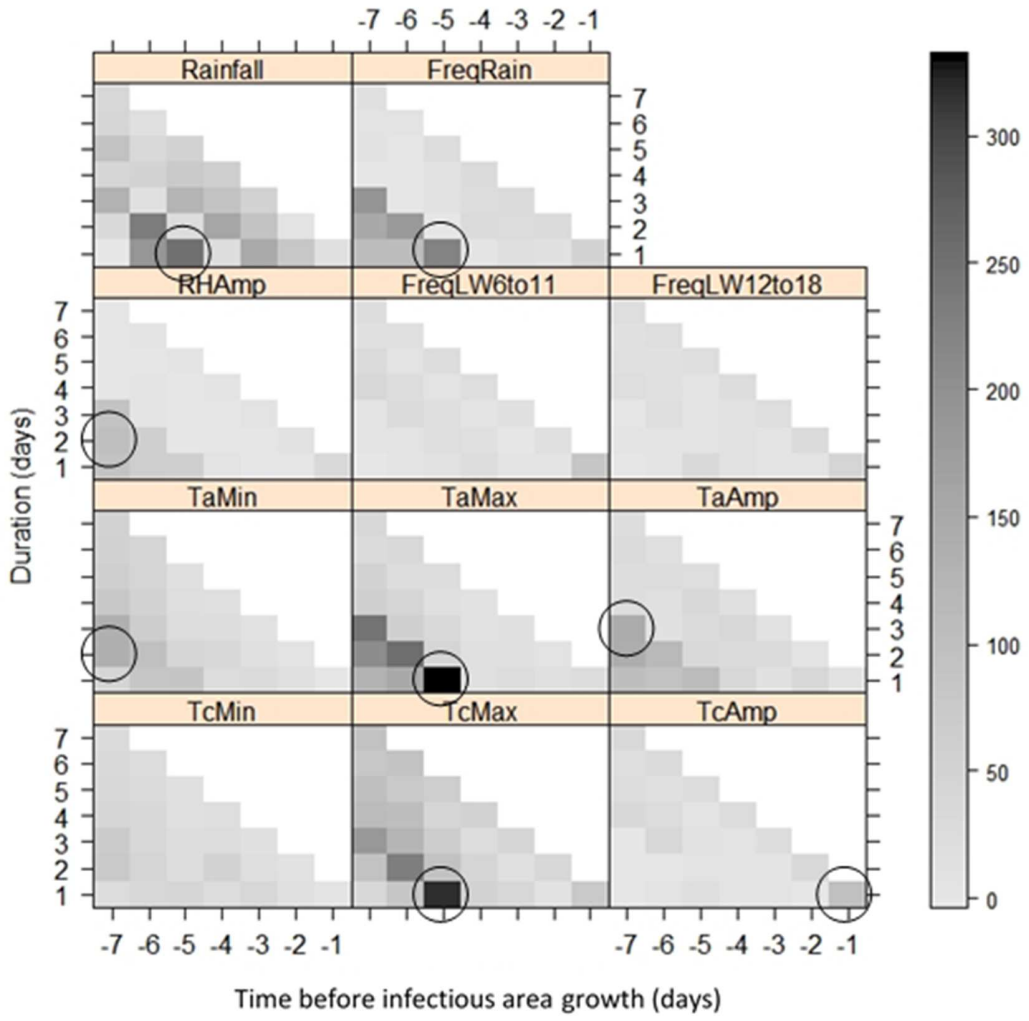

Fig. 6. Influence of microclimatic variables on lesion infectious area growth, per periods from one to seven days before the lesion infectious area growth (abscises) and for durations from one to seven days (ordinates). The scale on the right indicates the absolute difference between Akaike information criterion (AIC) of the model including the microclimatic variable averaged over the considered periods (dates and durations) (*InfectiousArea* ~ *InfectiousArea* $_{day\text{-}7}$ + *MicroclimVar* $_{period}$) and AIC of its reference model without including the microclimatic variable (*InfectiousArea* ~ *InfectiousArea* $_{day\text{-}7}$). The highest AIC differences, labelled with black circles, indicate the periods, to be considered for the microclimatic variable, that better explain lesion infectious area growth.

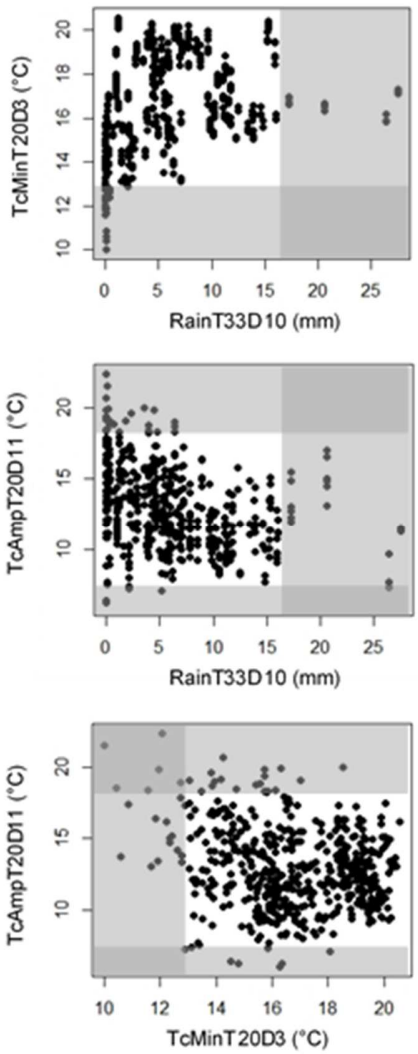

Fig. 7. Graphs displaying the distributions of the microclimatic variables used to develop the complete model forecasting the lesion emergence probability by foliar site. Grey areas are removed ranges due to under representation of data. $TcMin_{T20D3}$: averaged daily minimum leaf temperature over a period of three days starting 20 days before lesion emergence; $Rain_{T33D10}$: averaged daily rainfall over a period of 10 days starting 33 days before lesion emergence; $TcAmp_{T20D11}$: averaged daily amplitude of leaf temperature over a period of 11 days starting 20 days before lesion emergence.

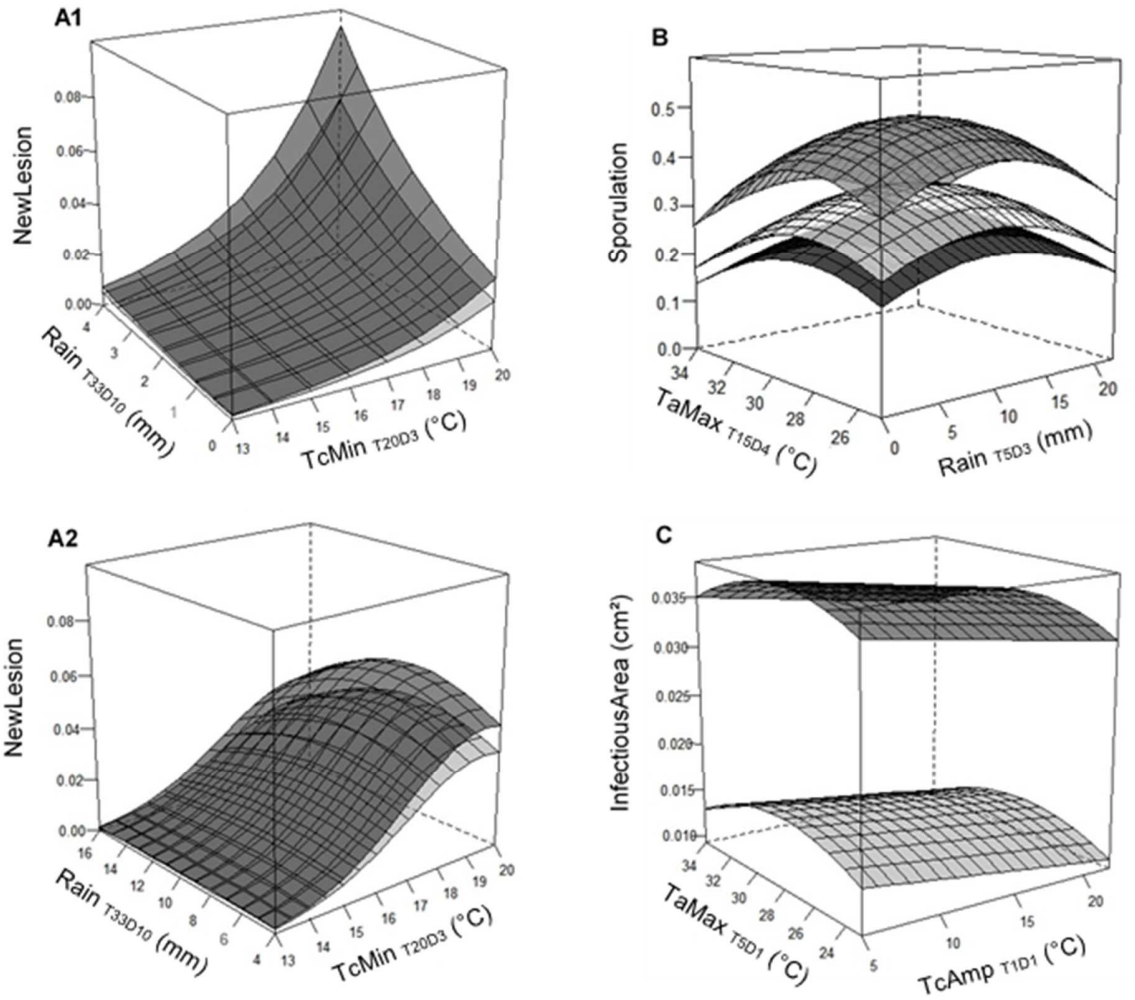

Fig. 8. Predictions of models A1 and A2 (graphs A1 and A2) for the lesion emergence probability of one of the 25 leaf sites considered, model B for sporulation probability (graph B) and model C for lesion infectious area growth (graph C). Graphs A1 and A2 were presented among model's variation ranges of $Rain_{T33D10}$ and $TcMin_{T20D3}$, while $TcAmp_{T20D11}$ (ranges [6.2:17.9] in model A1 and [7.1:17.3] in model A2) was fixed to its mean and *PastInoculum* (range [0:1.1] in model A1 and [0:3.8] in model A2) to its first (clear grey) and third quantiles (dark grey). Graph B was represented among variation ranges of $TaMin_{T15D4}$ and $Rain_{T5D3}$, while $Rain_{T12D2}$ (range [0:28.3]), $TcAmp_{T4D1}$ (range [5.9:18.9]) and *PlantFruitLoad* (range [0:1150]) were fixed to their mean and *LesionAge* (range [0:50]) was fixed to seven (clear grey), fifteen (grey) and 23 days (dark grey). Graph C was presented among variation ranges of $TaMax_{T5D1}$ and $TcAmp_{T1D1}$ and $InfectiousArea_{day\text{-}7}$ (range [0:0.295]) was fixed to its first (clear grey) and third quantiles (dark grey). All the variables are described in Tables 2 and 3.

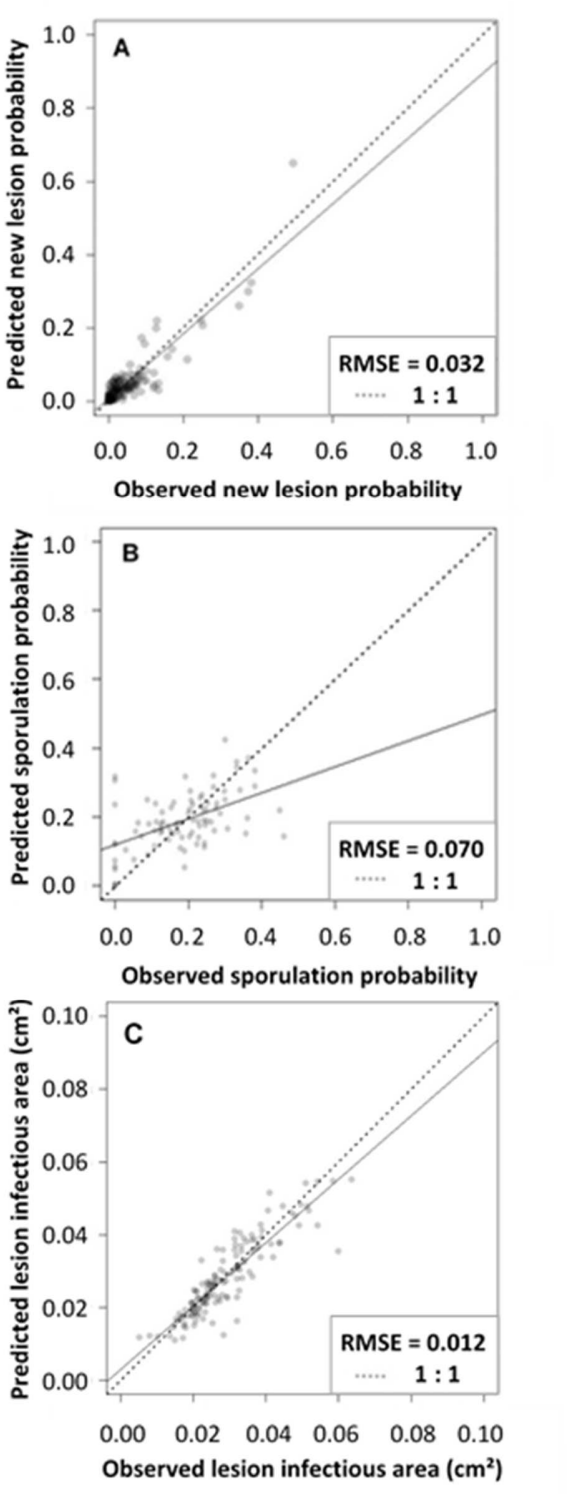

Fig. 9. Regressions between predicted values and observed averaged values by plot and date for new lesion emergence probability by foliar site (A), sporulation probability (B) and lesion infectious area (C).

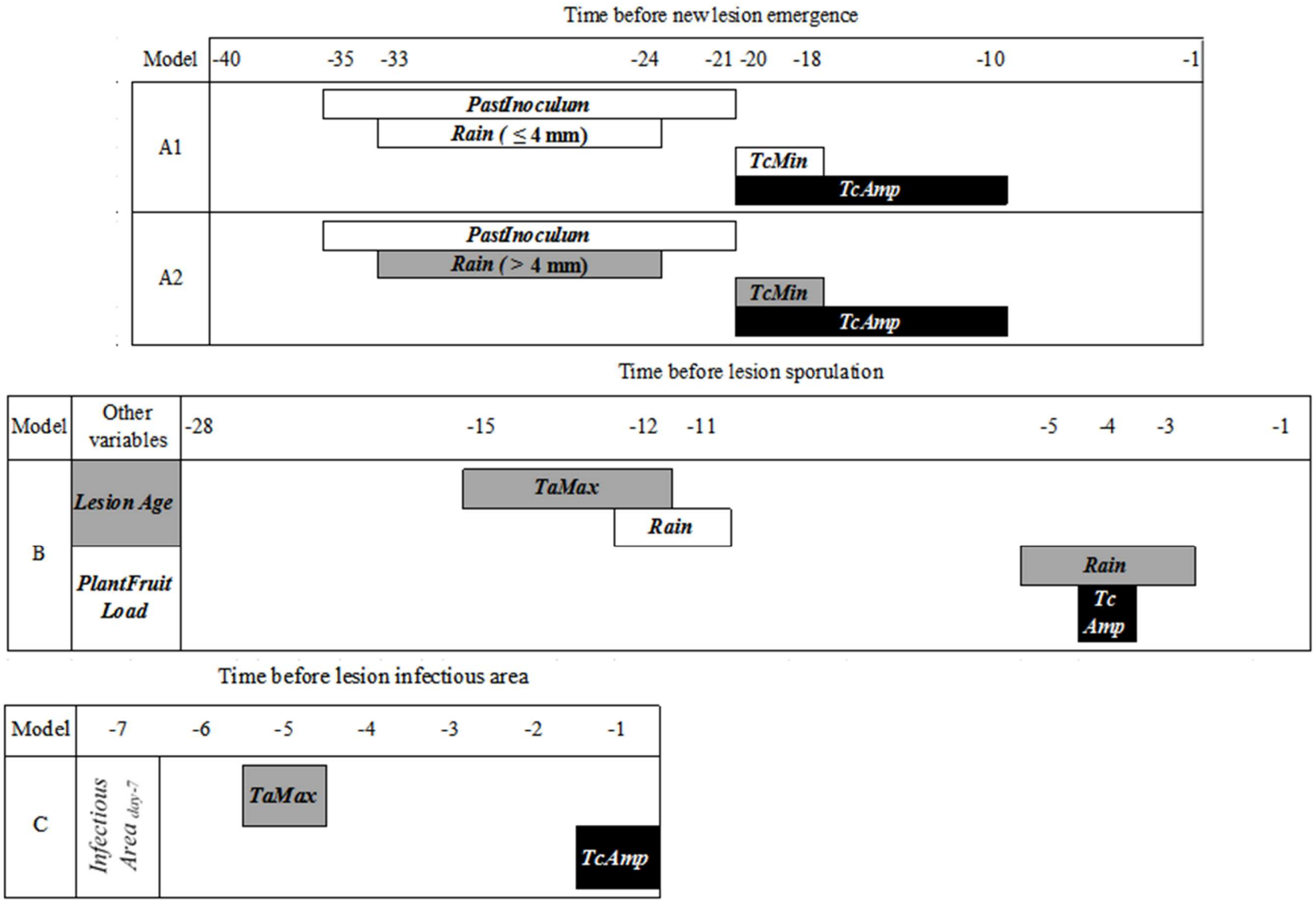

Fig. 10. Representations with a time axis of the variables corresponding to the complete models A1, A2, B and C. The box color of the variables indicates a positive effect (white), a negative effect (black) and a unimodal effect with a maximum (grey).

Table 1

Weather-based predictive models of coffee leaf rust development

Variable to forecast	Studied period for climatic variables	Number of tested variables			References
		Weather	Rust	Host and practices	
Latency period	Latency period	2	0	0	Rayner 1961 Kushalappa and Martins 1980 Santacreo et al. 1983 Tronconi et al. 1995
		2	0	1	de Moraes et al. 1976
Incubation period	Incubation period	2	0	0	Kushalappa and Martins 1980 Tronconi et al. 1995
Number of lesions per leaf	Over last 15, 30 or 45 days	3	0	1	Alfonsi et al. 1974
Proportion of rust area	Over the last 40 days	1	2	0	Kushalappa and Chaves 1980
Apparent infection rate over 28 days	Over last 14 days or from 28 to 14 days before	4	2	1	Kushalappa 1981
	Semi-mechanistic approach	4	2	1	Kushalappa et al. 1983
		4	2	2	Kushalappa et al. 1984 Holguín 1987
Apparent infection rate over 15 days	Over last 15 days	5	0	0	Pedro 1983
Incidence	Over last 15, 30, 45 or 60 days	8	0	1	Pinto et al. 2002
	Over the year	1	1	> 40	Avelino et al. 2006
Class of monthly incidence variations	Latency period	> 10	0	2	Meira et al. 2008
		> 10	0	1	Meira et al. 2009
		> 10	1	1	Cintra et al. 2011
Class of incidence	Over last 45 days	> 10	1	2	Luaces et al. 2010
		> 20	1	2	Perez Ariza et al. 2012
	Last month and last two months	6	0	7	Corrales et al. 2015, 2016
Month average of daily infection risk	Mechanistic approach	2	0	0	Bebber et al. 2016
Apparent infection rate over 30 days	Periods of 30 days, 90 days before, 60 days before and 30 days before	> 10	0	2	Hinnah et al. 2018
Incidence	Last 28 days	4	0	6	Liebig et al., 2019

Table 2

Description of the three forecasted variables on rust development and their explanatory variables including microclimatic descriptors

Dependent variables	Description	Unit	Range
NewLesion	Presence/absence of a new rust lesion per leaf site	-	0 or 1
Sporulation	Presence/absence of uredospores on each rust lesion	-	0 or 1
InfectiousArea	Area with uredospores per lesion	cm^2	[0.001;0.535]
Explanatory variables	**Description**	**Unit**	**Range**
Inoculum	Area with uredospores per branch averaged per plot	cm^2	[0;3.9]
LesionAge	Time since the lesion emergence	days	0, 7, 14, 21, 28, 35, 42, 49
$InfectiousArea_{day-7}$	Past area with uredospores per lesion (7 days ago)	cm^2	[0.001;0.295]
LeafStratum	Coffee leaf stratum (Bottom; Middle; Top)	-	-
PlantFruitLoad	Plant fruiting nodes	-	[0;1793]
Rainfall	Daily rainfall	mm	[0;186.9]
FreqRain	Daily number of rainy hours	-	[0;24]
TaMin	Daily minimum air temperature	°C	[7.5;21.9]
TaMax	Daily maximum air temperature	°C	[15.5;35.9]
TaAmp	Daily amplitude of air temperature	°C	[1.9;22.9]
RHAmp	Daily amplitude of relative humidity	%	[0;87.8]
TcMin	Daily minimum leaf temperature	°C	[8.4;22.0]
TcMax	Daily maximum leaf temperature	°C	[15.5;41.3]
TcAmp	Daily amplitude of leaf temperature	°C	[1.6;28.8]
FreqLW6to11	Leaf wetness duration from 6am to 11am	h	[0;6]
FreqLW12to18	Leaf wetness duration from 12am to 6pm	h	[0;7]

Table 3

Microclimatic variables identified as the most explicative for each of the three models of rust development. The variables in bold are the ones conserved after removing the over-correlated variables ($r > 0.7$) and those underlined are the variables used in the full models.

Model	Microclimatic variables identified			
Lesion emergence probability	$TaMin_{T11D1}$ $TaMin_{T19D2}$ $TaMin_{T44D3}$ $TaMax_{T9D2}$ $TaMax_{T23D3}$ $TaMax_{T32D6}$ $TaMax_{T44D6}$	$TcMin_{T11D1}$ **$\underline{TcMin_{T20D3}}$** $TcMin_{T28D25}$ $TcMin_{T37D3}$ $TcMin_{T44D3}$ $TcMin_{T50D17}$ $TcAmp_{T11D2}$ **$\underline{TcAmp_{T20D11}}$**	$Rain_{T16D6}$ $Rain_{T26D3}$ **$\underline{Rain_{T33D10}}$** $Rain_{T35D17}$ $Rain_{T42D19}$	$FreqLW6to11_{T13D3}$ $FreqLW6to11_{T13D12}$ $FreqLW6to11_{T20D11}$ $FreqLW6to11_{T37D5}$ $FreqLW12to18_{T13D10}$ $FreqLW12to18_{T19D16}$
Sporulation probability	$TaMin_{T14D1}$ $TaMin_{T22D3}$ $TaMin_{T25D7}$ $TaMax_{T4D1}$ **$\underline{TaMax_{T15D4}}$** $TaMax_{T23D4}$ $TaMax_{T23D12}$	$TcMin_{T14D1}$ $TcMin_{T22D3}$ $TcMin_{T25D6}$ $TcMax_{T4D1}$ $TcMax_{T15D4}$ **$\underline{TcAmp_{T4D1}}$** **$TcAmp_{T13D2}$**	**$\underline{Rain_{T5D3}}$** **$\underline{Rain_{T12D2}}$** **$Rain_{T17D5}$** $Rain_{T26D4}$	$FreqLW6to11_{T13D2}$ $FreqLW12to18_{T5D2}$ **$FreqLW12to18_{T18D3}$** $FreqRain_{T3D1}$ $FreqRain_{T12D10}$
Lesion infectious area	**$TaMin_{T7D2}$** **$\underline{TaMax_{T5D1}}$**	$TaAmp_{T7D3}$ $TcMax_{T5D1}$	**$\underline{TcAmp_{T1D1}}$** $RHAmp_{T7D2}$	$Rain_{T5D1}$ $FreqRain_{T5D1}$

Microclimatic variables (MV): TaMin; TaMax; TaAmp: TcMin: TcMax; TcAmp; RHAmp; FreqLW6to11; FreqLW12to18 are described in Table 2 and Rain is a shorter term for Rainfall

MV_{TxDy}: averaged daily microclimatic variable over a y-days period starting x days before the symptom or sign onset

Table 4

Description of the parameters estimate of the models A1, A2, B and C

Model	Parameter	Value [±Standard error]	Unit
A1	$\alpha_{1.1}$	- 11.41 [±0.22]	-
	$\alpha_{1.2}$	+ 1.84 [±0.065]	cm^{-2}
	$\alpha_{1.3}$	+ 0.33 [±0.015]	mm^{-1}
	$\alpha_{1.4}$	+ 0.38 [±0.0099]	$°C^{-1}$
	$\alpha_{1.5}$	- 0.017 [±0.0089]	$°C^{-1}$
A2	$\alpha_{2.1}$	- 32.57 [±1.22]	-
	$\alpha_{2.2}$	+ 1.15 [±0.010]	cm^{-2}
	$\alpha_{2.3}$	+ 0.16 [±0.015]	mm^{-1}
	$\alpha_{2.4}$	- 0.0091 [±0.00077]	mm^{-2}
	$\alpha_{2.5}$	+ 3.08 [±0.14]	$°C^{-1}$
	$\alpha_{2.6}$	- 0.079 [±0.0039]	$°C^{-2}$
	$\alpha_{2.7}$	- 0.10 [±0.0043]	$°C^{-1}$
B	β_1	- 19.69 [±2.11]	-
	β_2	+ 0.30 [±0.0047]	$days^{-1}$
	β_3	- 0.010 [±0.00021]	$days^{-2}$
	β_4	+ 0.00016 [±0.000044]	-
	β_5	+ 1.24 [±0.14]	$°C^{-1}$
	β_6	- 0.022 [±0.0024]	$°C^{-2}$
	β_7	+ 0.018 [±0.0019]	mm^{-1}
	β_8	+ 0.065 [±0.0070]	mm^{-1}
	β_9	- 0.0032 [±0.00037]	mm^{-2}
	β_{10}	- 0.045 [±0.0043]	$°C^{-1}$
C	γ_1	- 0.068 [±0.0081]	-
	γ_2	+ 1.30 [±0.0045]	cm^{-2}
	γ_3	+ 0.0057 [±0.00057]	$°C^{-1}$
	γ_4	- 0.00010 [±0.000010]	$°C^{-2}$
	γ_5	- 0.00021 [±0.000030]	$°C^{-1}$